electron Beam Polarimetry
Day 2

Ciprian Gal

With loads of borrowed materials from Dave Gaskell, Allison Zec and others

Jefferson Lab

References

- CFNS Workshop on Beam Polarization and Polarimetry
  - https://indico.bnl.gov/event/7583/
- EICUG Working Group on Polarimetry and Ancillary Detectors (luminosity monitor)
  - https://indico.bnl.gov/category/280/
- Precision electron beam polarimetry for next generation nuclear physics experiments
  - *Int.J.Mod.Phys.E* 27 (2018) 07, 1830004, https://doi.org/10.1142/S0218301318300047
- “Conceptual Design Report of a Compton Polarimeter for Cebaf Hall A”, https://hallaweb.jlab.org/compton/Documentation/Technical/1996/proposal.ps.gz

Recap

$$A = \frac{\text{condition1} - \text{condition2}}{\text{condition1} + \text{condition2}}$$

$$A_{\parallel} = \frac{1}{P_e P_h}\left[\frac{N^{++} - RN^{+-}}{N^{++} + RN^{+-}}\right]$$

```
: hbarc = 1.9732858E-11
  pi = 3.141592653589793
  laser_lambda = 532e-7
  E_laser = hbarc*2*pi/laser_lambda
  print("photon energy = ",E_laser)

  photon energy =  2.3305489371101722e-06
```

$$A_{\text{measured}} = P_{\text{beam}} A_{\text{effective}}$$

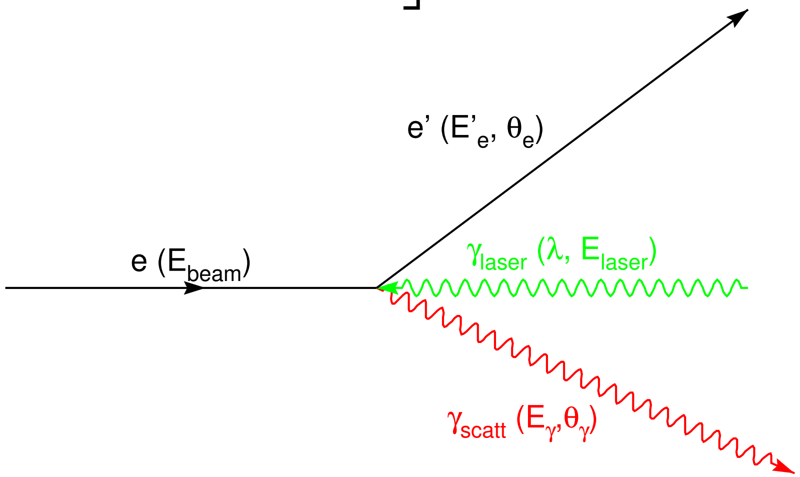

$$\gamma = E_{beam}/me_{lectron}$$

$$E_\gamma \approx E_{\text{laser}} \frac{4a\gamma^2}{1 + a\theta_\gamma^2\gamma^2}$$

$$a = \frac{1}{1 + 4\gamma E_{\text{laser}}/m_e}$$

<u>For green laser (532 nm):</u>

→ E_γ^{max} ~ 34.5 MeV at E_{beam}=1 GeV

→ E_γ^{max} = 3.1 GeV at E_{beam}=11 GeV

Recap

$$A = \frac{\text{condition1} - \text{condition2}}{\text{condition1} + \text{condition2}}$$

$$A_{\parallel} = \frac{1}{P_e P_h}\left[\frac{N^{++} - RN^{+-}}{N^{++} + RN^{+-}}\right]$$

```
hbarc = 1.9732858E-11
pi = 3.141592653589793
laser_lambda = 532e-7
E_laser = hbarc*2*pi/laser_lambda
print("photon energy = ",E_laser)
```

```
photon energy =  2.3305489371101722e-06
```

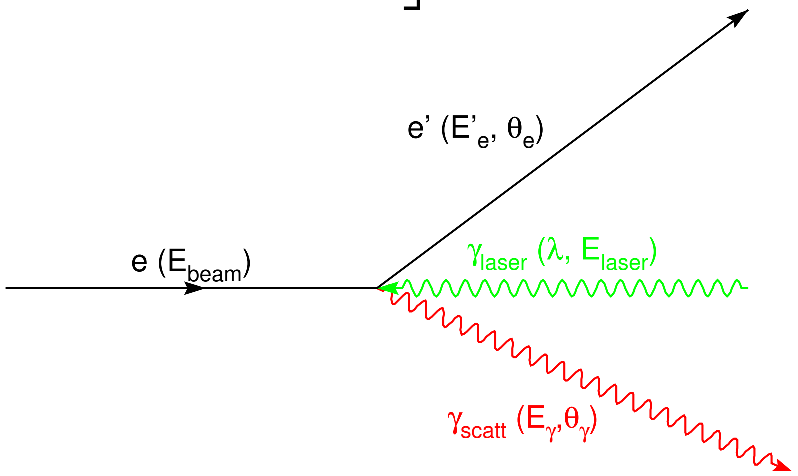

$$A_{\text{measured}} = P_{\text{beam}} A_{\text{effective}}$$

$$\gamma = E_{beam}/me_{lectron}$$

$$E_\gamma \approx E_{\text{laser}} \frac{4a\gamma^2}{1 + a\theta_\gamma^2\gamma^2}$$

$$a = \frac{1}{1 + 4\gamma E_{\text{laser}}/m_e}$$

<u>For green laser (532 nm):</u>

→ E_γ^{max} ~ 34.5 MeV at E_{beam}=1 GeV

→ E_γ^{max} = 3.1 GeV at E_{beam}=11 GeV

Compton spectrum

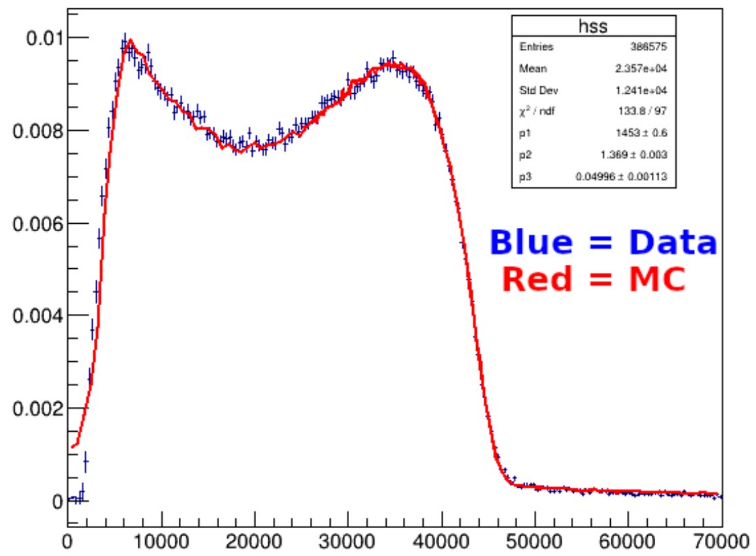

Scattered photon cone

Calculate the angle for which the scattered photon energy is half of the maximum energy:

In [5]:
```
Theta_half = np.sqrt(1/(a*gamma**2))
print("E_g_max/2 angle (deg) = ",Theta_half*180/pi)
```

```
E_g_max/2 angle (deg) =  0.006356700858973076
```

Calculate the radial position of this photon 30 meters from the interaction region:

In [6]:

Scattered photon cone

Calculate the angle for which the scattered photon energy is half of the maximum energy:

In [5]:
```
Theta_half = np.sqrt(1/(a*gamma**2))
print("E_g_max/2 angle (deg) = ",Theta_half*180/pi)
```

```
E_g_max/2 angle (deg) =  0.006356700858973076
```

Calculate the radial position of this photon 30 meters from the interaction region:

In [6]:
```
cone_size_30m = np.tan(Theta_half)*3000
print("R after 30 m = ",cone_size_30m,"cm")
```

```
R after 30 m =  0.3328360800259083 cm
```

Compton cross - sections

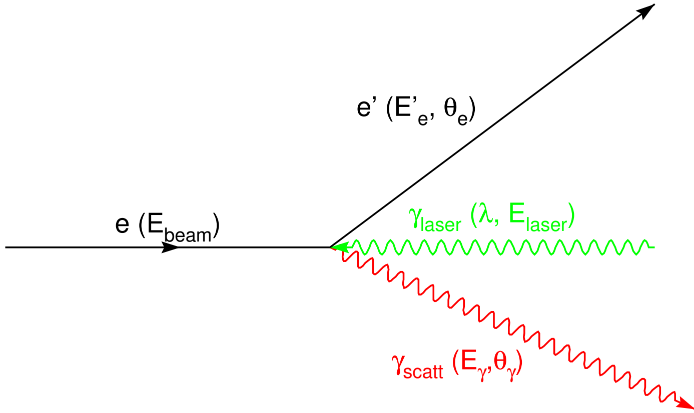

$$\frac{d\sigma}{d\rho} = 2\pi r_0^2 a \left[\frac{\rho^2(1-a^2)}{1-\rho(1-a)} + 1 + \left(\frac{1-\rho(1+a)}{1-\rho(1-a)} \right)^2 \right]$$

r_0 = classical electron radius

```
print("Cross section for half energy = ", compton_xsec(0.5))
```

```
Cross section for half energy =  4.288483334832458e-25
```

Compton cross - sections

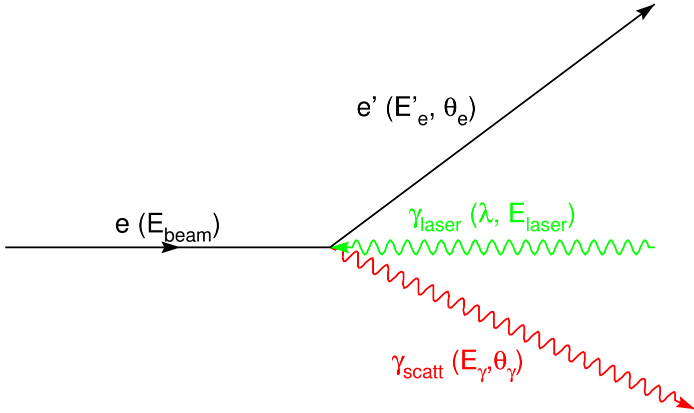

$$\frac{d\sigma}{d\rho} = 2\pi r_0^2 a \left[\frac{\rho^2(1-a^2)}{1-\rho(1-a)} + 1 + \left(\frac{1-\rho(1+a)}{1-\rho(1-a)} \right)^2 \right]$$

r_0 = classical electron radius

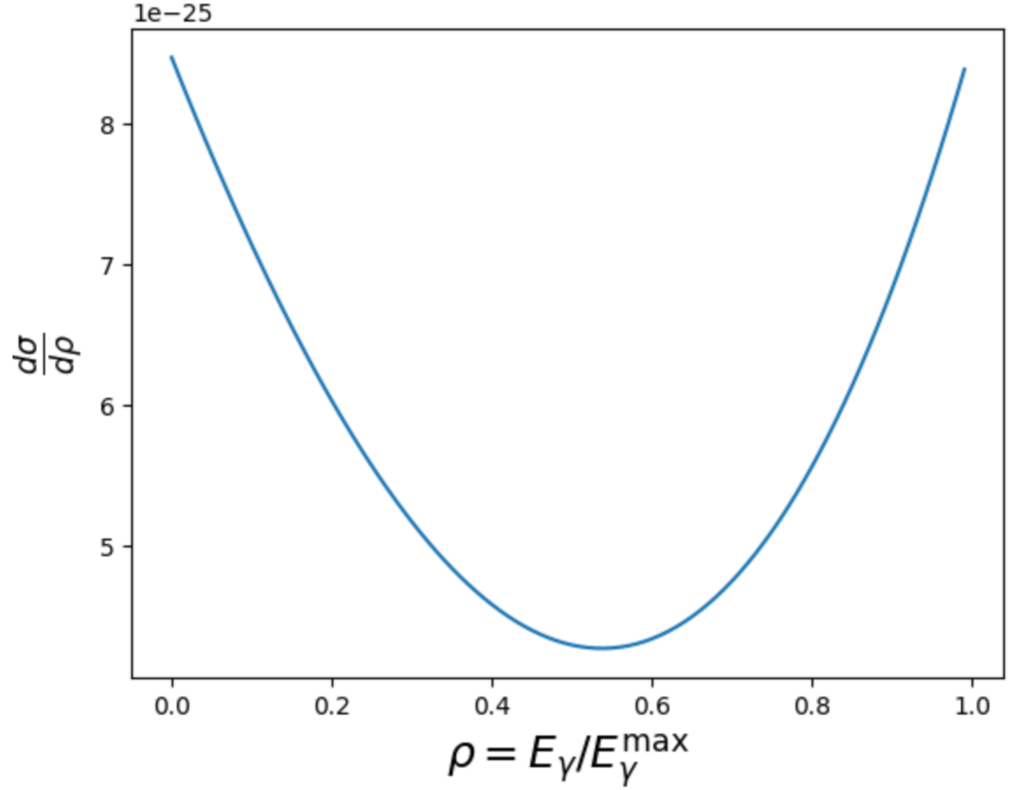

Analyzing power: longitudinal

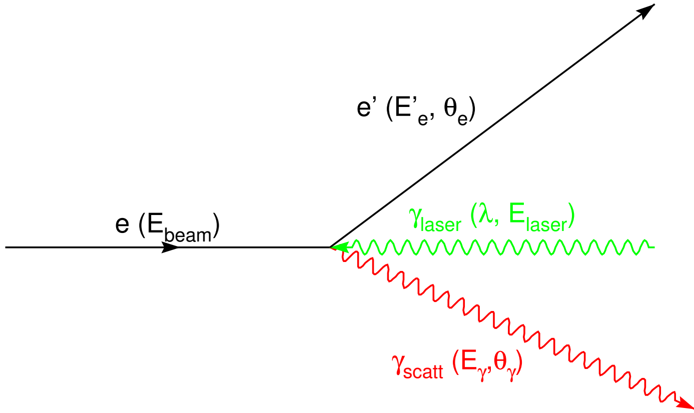

$$A_{\text{long}} = \frac{2\pi r_o^2 a}{(d\sigma/d\rho)}(1-\rho(1+a))\left[1-\frac{1}{(1-\rho(1-a))^2}\right]$$

```
print("Longitudinal asymmetry for half energy = ", compton_A_long(0.5))
Longitudinal asymmetry for half energy =  -0.01275548205649403
```

Analyzing power: longitudinal

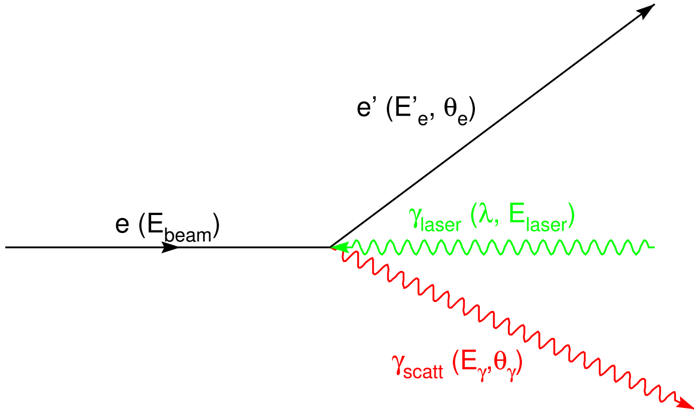

$$A_{\rm long} = \frac{2\pi r_o^2 a}{(d\sigma/d\rho)}(1-\rho(1+a))\left[1-\frac{1}{(1-\rho(1-a))^2}\right]$$

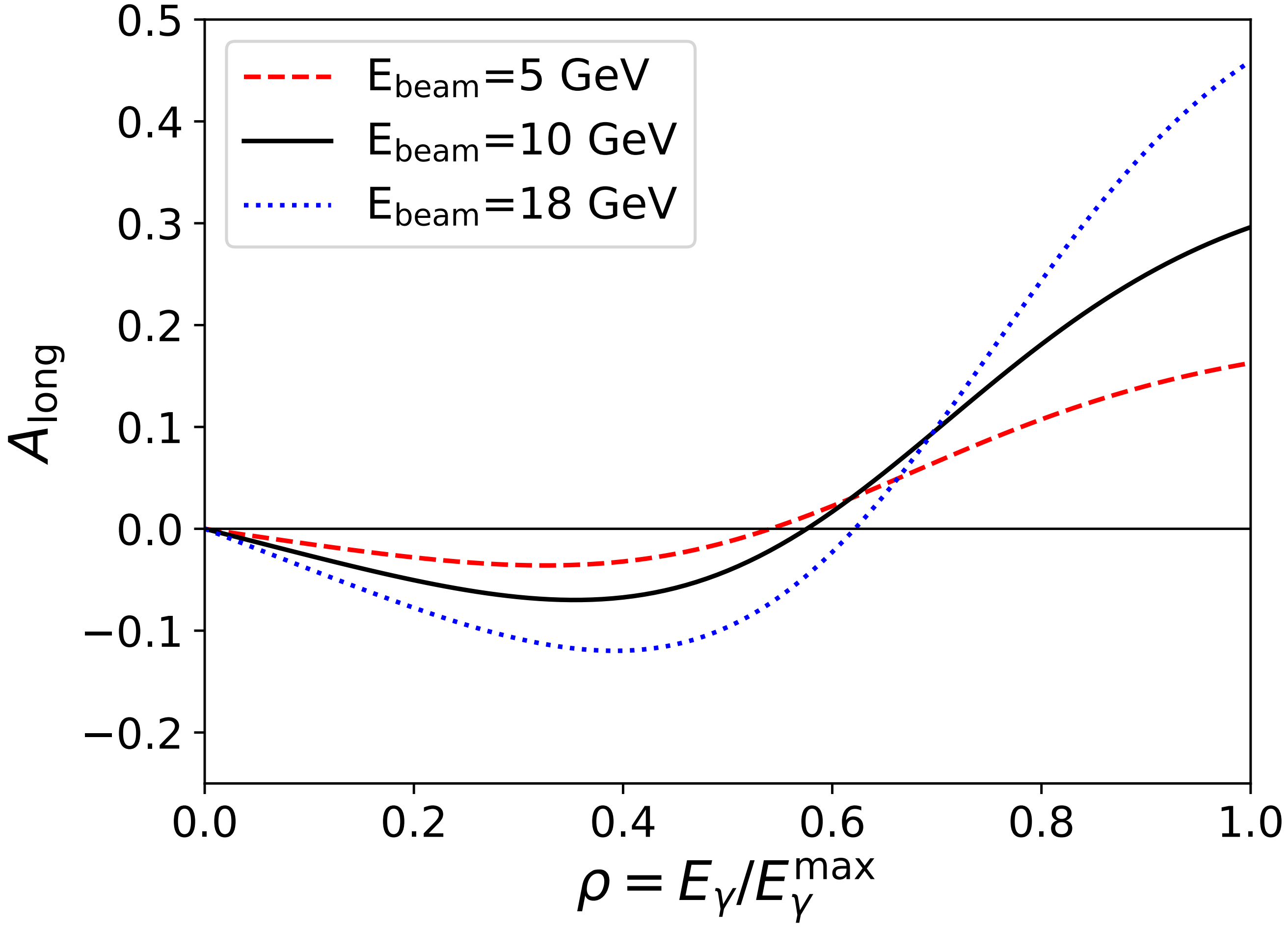

Analyzing power: transverse

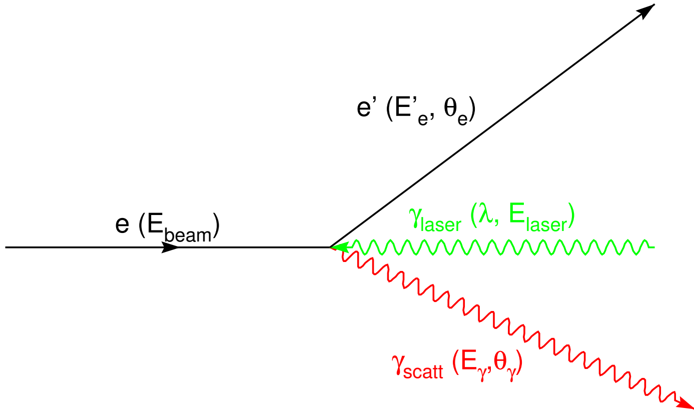

$$A_{\mathrm{T}} = \frac{2\pi r_o^2 a}{(d\sigma/d\rho)} \cos\phi \left[\rho(1-a)\frac{\sqrt{4a\rho(1-\rho)}}{(1-\rho(1-a))}\right]$$

```
print("Transverse asymmetry for half energy = ", compton_A_perp(0.5))
```

```
Transverse asymmetry for half energy =  0.07451809329701582
```

Analyzing power: transverse

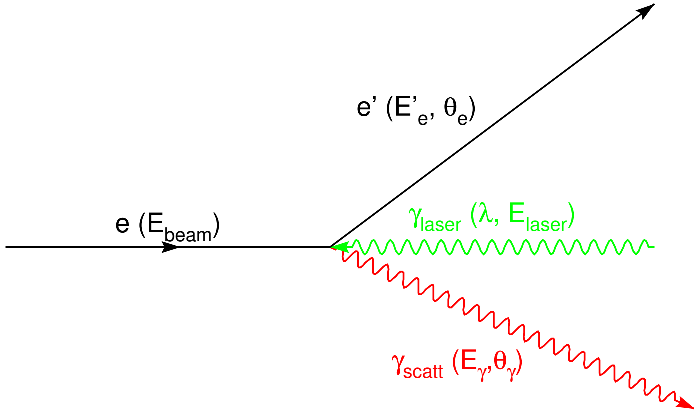

$$A_{\mathrm{T}} = \frac{2\pi r_o^2 a}{(d\sigma/d\rho)} \cos\phi \left[\rho(1-a) \frac{\sqrt{4a\rho(1-\rho)}}{(1-\rho(1-a))} \right]$$

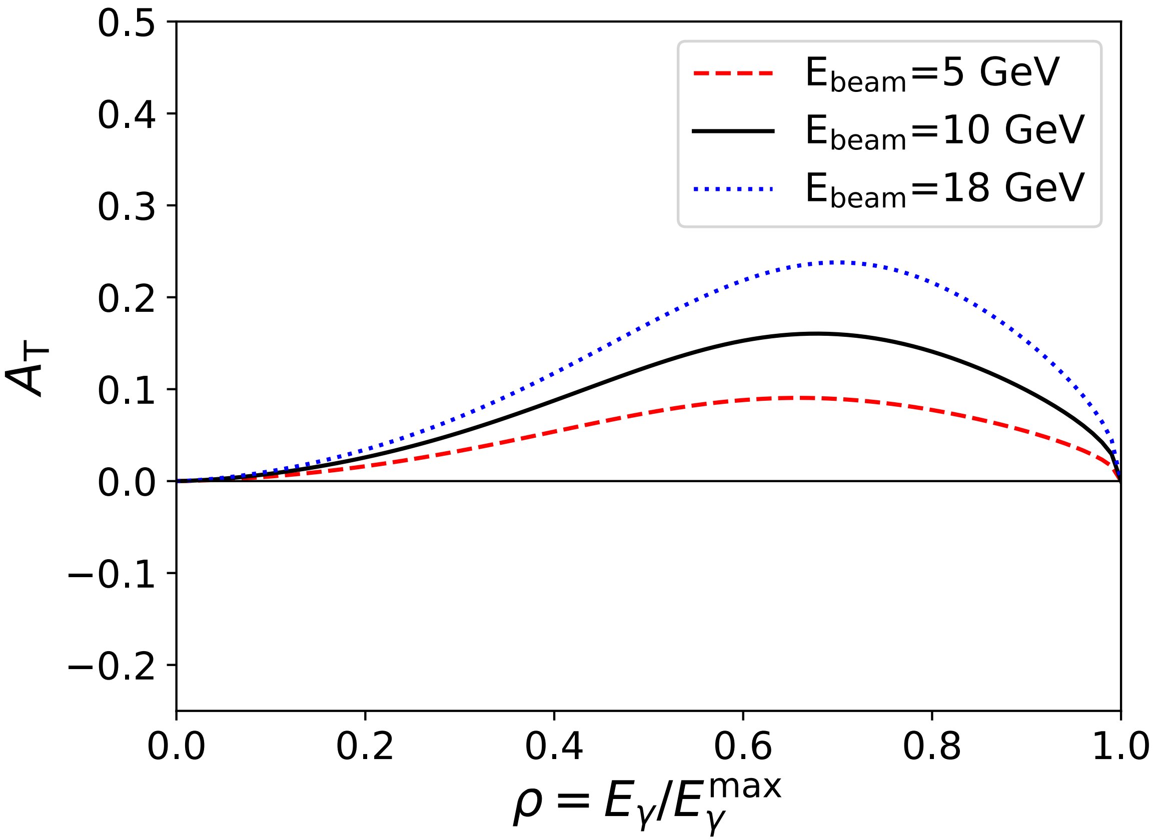

Implementation

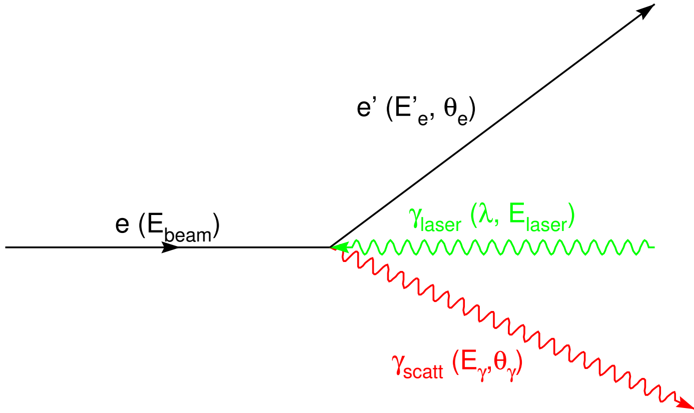

- Design interaction region

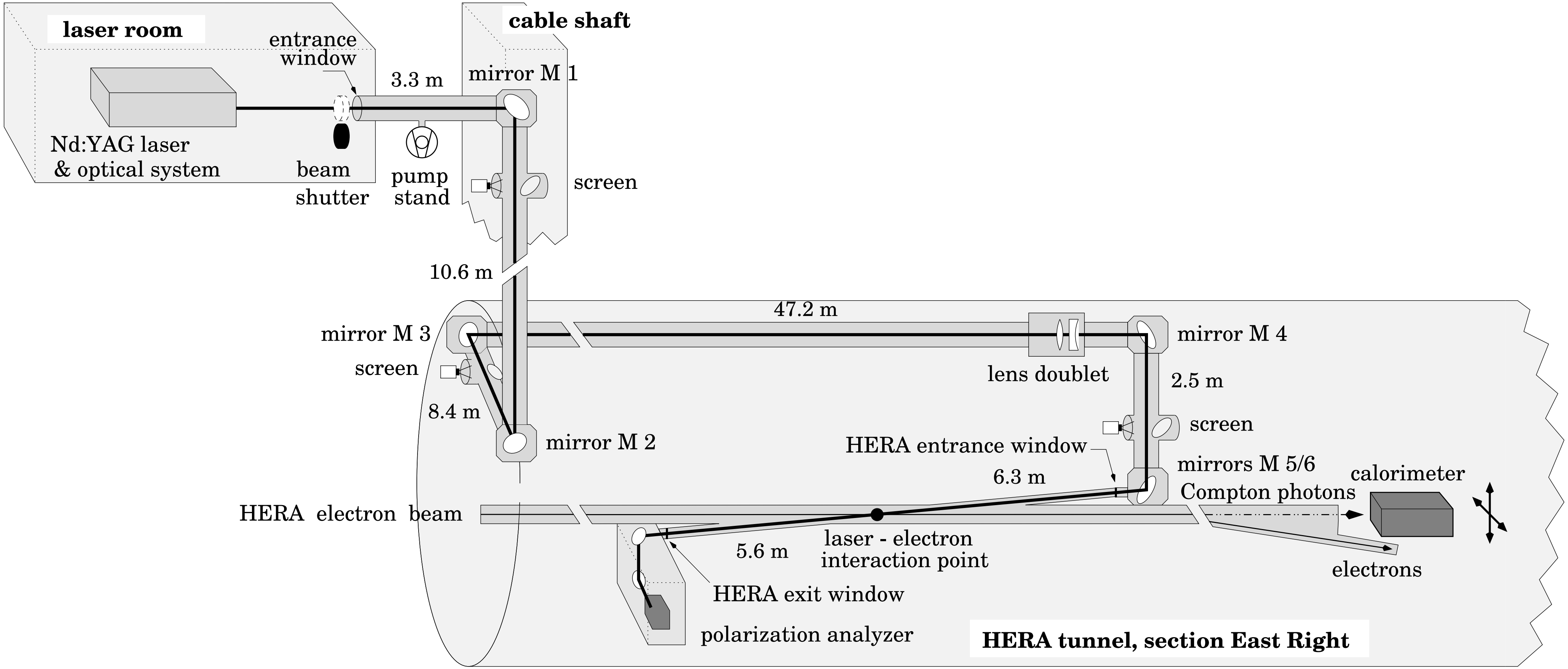

Luminosity and x-ing angle

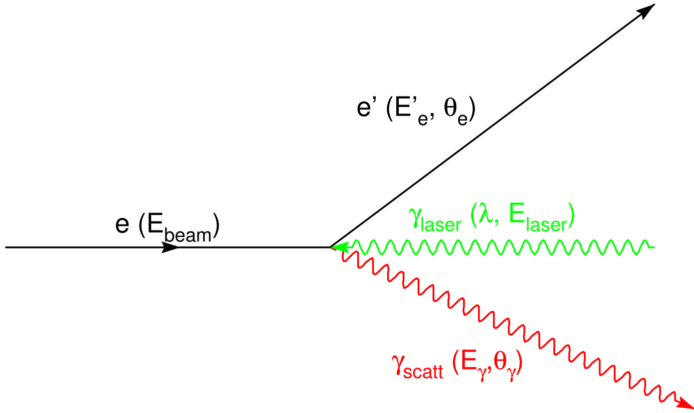

- $N_{\gamma(e)}$ = number of photons (electrons) per bunch
- Assumes beam sizes constant over region of overlap (ignores "hourglass effect")
- Beam size at interaction point with laser dictates luminosity (for given beam current and laser/electron beam crossing angle)

Luminosity for CW laser colliding with electron beam at non-zero crossing angle:

$$\mathcal{L} = \frac{(1+\cos\alpha_c)}{\sqrt{2\pi}} \frac{I_e}{e} \frac{P_L \lambda}{hc^2} \frac{1}{\sqrt{\sigma_e^2 + \sigma_\gamma^2}} \frac{1}{\sin\alpha_c}$$

```
print('Luminosity for CW laser/beam (small crossing angle): ', LumiCW)
```

```
Luminosity for CW laser/beam (small crossing angle):  7.033923214036582e+30
```

Pulsed laser:

$$\mathcal{L} = f_{coll} N_\gamma N_e \frac{\cos(\alpha_c/2)}{2\pi} \frac{1}{\sqrt{\sigma_{x,\gamma}^2 + \sigma_{x,e}^2}} \frac{1}{\sqrt{(\sigma_{y,\gamma}^2 + \sigma_{y,e}^2)\cos^2(\alpha_c/2) + (\sigma_{z,\gamma}^2 + \sigma_{z,e}^2)\sin^2(\alpha_c/2)}}$$

```
Luminosity for one pulse (small crossing angle):  1.314609642805983e+24
Luminosity for Pulsed laser/beam (small crossing angle):  1.314609642805983e+32
Luminosity for Pulsed laser colliding with one beam bunch (small crossing angle):  1.0253955213886668e+29
```

Luminosity and x-ing angle

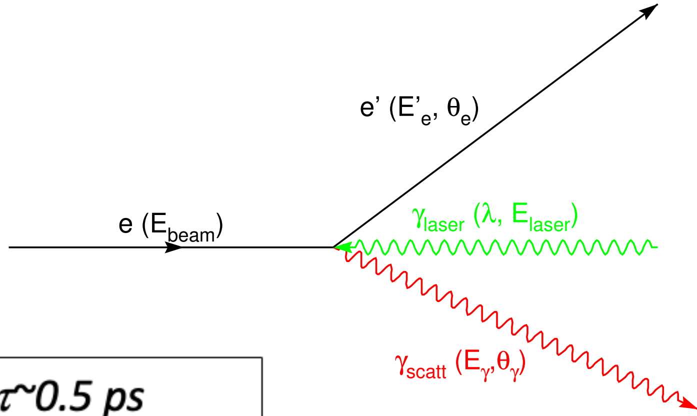

Pulsed laser provides higher luminosity than CW lasers (for pulsed beams)

→ As crossing angle gets smaller, improvement in rates become more comparable

→ Main advantage at small crossing angle in using pulsed laser is identification of beam bunch and ability to measure polarization profile

→ Laser beam bunch length smaller than beam bunch will allow extraction of polarization vs. time in bunch (center vs. tails)

JLab beam → 499 MHz, $\Delta\tau$~0.5 ps

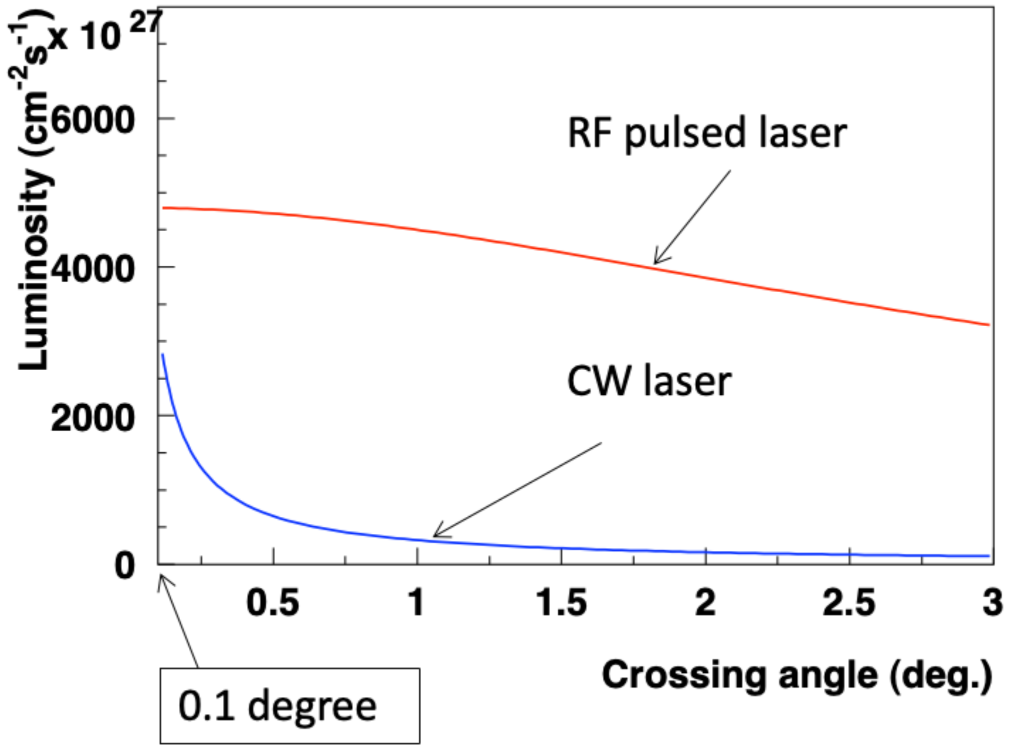

Photon rates

Calculate the rate of scattered photons for a single bunch collision asumming a $\rho_{min} = E_{laser}/E_{\gamma max}$:

$$L = \frac{1}{\sigma}\frac{dN}{dt}.$$

Calculate the rate of scattered photons for a single bunch collision asumming a $\rho_{min} = E_{laser}/E_{\gamma max}$:

In [ ]:

```
LumiOneBunch=1.3416E24
fcoll=78000
rhomin = E_laser/E_g_max
xsect = integrate.quad(lambda rho: compton_xsec(rho),rhomin,1.0)
### Your code goes here
```

Photon rates

Calculate the rate of scattered photons for a single bunch collision asumming a $\rho_{min} = E_{laser}/E_{\gamma max}$:

$$L = \frac{1}{\sigma}\frac{dN}{dt}.$$

Calculate the rate of scattered photons for a single bunch collision asumming a $\rho_{min} = E_{laser}/E_{\gamma max}$:

In [21]:
```
fcoll = 78000
LumiOneBunch = 1.314609642805983e+24
rhomin = E_laser/E_g_max
xsect = integrate.quad(lambda rho: compton_xsec(rho),rhomin,1.0)
rate = xsect[0]*LumiOneBunch*fcoll
print('Backscattered photon rate (Hz)', rate)
```

```
Backscattered photon rate (Hz) 58336.933178552485
```

Measurement time

Measurement time depends on luminosity, analyzing power, and measurement technique

$$t^{-1} = \mathcal{L}\sigma \left(\frac{\Delta P}{P}\right)^2 A^2_{method}$$

Average analyzing power:	$A^2_{method} = \langle A \rangle^2$	→ Average value of asymmetry over acceptance
Energy-weighted:	$A^2_{method} = \left(\frac{\langle EA \rangle}{\langle E \rangle}\right)^2$	→ Energy deposited in detector for each helicity state
Differential:	$A^2_{method} = \langle A^2 \rangle$	→ Measurement of asymmetry bin-by-bin vs. energy, etc.

$$\langle A \rangle^2 < \left(\frac{\langle EA \rangle}{\langle E \rangle}\right)^2 < \langle A^2 \rangle$$

Measurement times

Using the longitudinal asymmetry function from above calculate the average asymmetry and the time it takes to reach 1% statistical precision for this measurement:

$$t^{-1} = \mathcal{L}\sigma \left(\frac{\Delta P}{P}\right)^2 A^2_{method}$$

Measurement times

Using the longitudinal asymmetry function from above calculate the average asymmetry and the time it takes to reach 1% statististical precision for this measurement:

$$t^{-1} = \mathcal{L}\sigma \left(\frac{\Delta P}{P}\right)^2 A^2_{method}$$

In [16]:
```
dP=0.01
P=0.8
num = integrate.quad(lambda rho: compton_A_long(rho)*compton_xsec(rho),rhomin,1.0)
A_avg = num[0]/xsect[0]
t_avg = 1.0/(rate*dP**2*P**2*A_avg**2)
print('Average longitudinal asymmetry: ', A_avg)
print('Time for 1% measurement (s): ', t_avg)
```

```
Average longitudinal asymmetry:  0.03427976755269462
Time for 1% measurement (s):  227.929582570587
```

Time estimations: longitudinal

$$t_{meth} = \left(\mathcal{L}\,\sigma_{\mathrm{Compton}}\;\mathrm{P_e^2 P_\gamma^2}\left(\frac{\Delta \mathrm{P_e}}{\mathrm{P_e}}\right)^2 \mathrm{A^2_{meth}}\right)^{-1}$$

A_{meth}

Single-photon	**Integrating**	**Energy Integrating**
$\langle \mathrm{A}^2 \rangle$	$\langle \mathrm{A} \rangle^2$	$\dfrac{\langle \mathrm{E}\cdot\mathrm{A}\rangle^2}{\langle \mathrm{E}^2\rangle}$

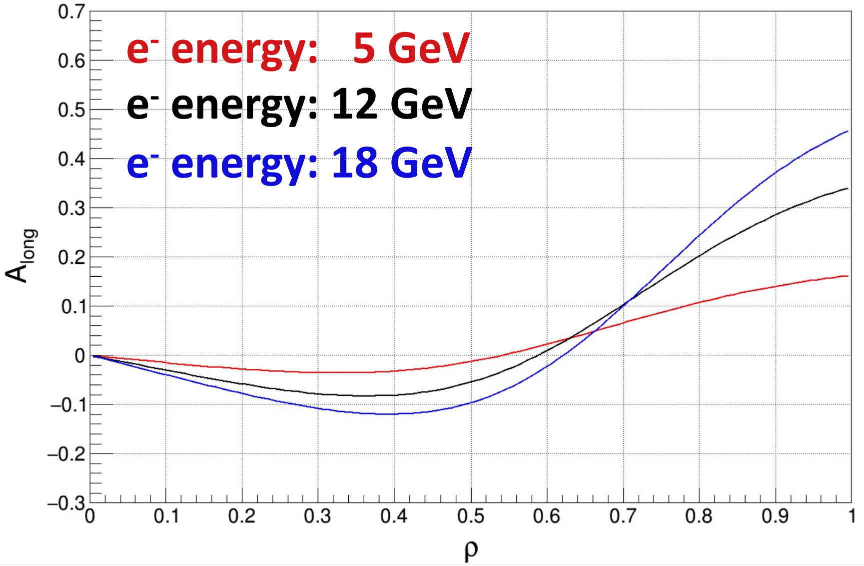

beam energy [GeV]	$\langle A^2_{\mathrm{long}}\rangle$	t[s]	$\langle A_{\mathrm{long}}\rangle^2$	time [ms]	$\frac{\langle \mathrm{E\cdot A}\rangle^2}{\langle \mathrm{E}^2\rangle}$	time [ms]
5	0.0061	29	0.0012	166	0.0022	88
12	0.0244	7	0.0033	69	0.0064	36
18	0.0414	4	0.0041	63	0.0085	30

- Differential measurement assumes 1 photon/electron per crossing
  - The power needed for the laser system is approximately 1W
- The integrated method accepts the entire luminosity of the pulsed system (note the change in unit)

Transverse asymmetry

$$A_{\mathrm{T}} = \frac{2\pi r_o^2 a}{(d\sigma/d\rho)} \cos\phi \left[\rho(1-a) \frac{\sqrt{4a\rho(1-\rho)}}{(1-\rho(1-a))} \right]$$

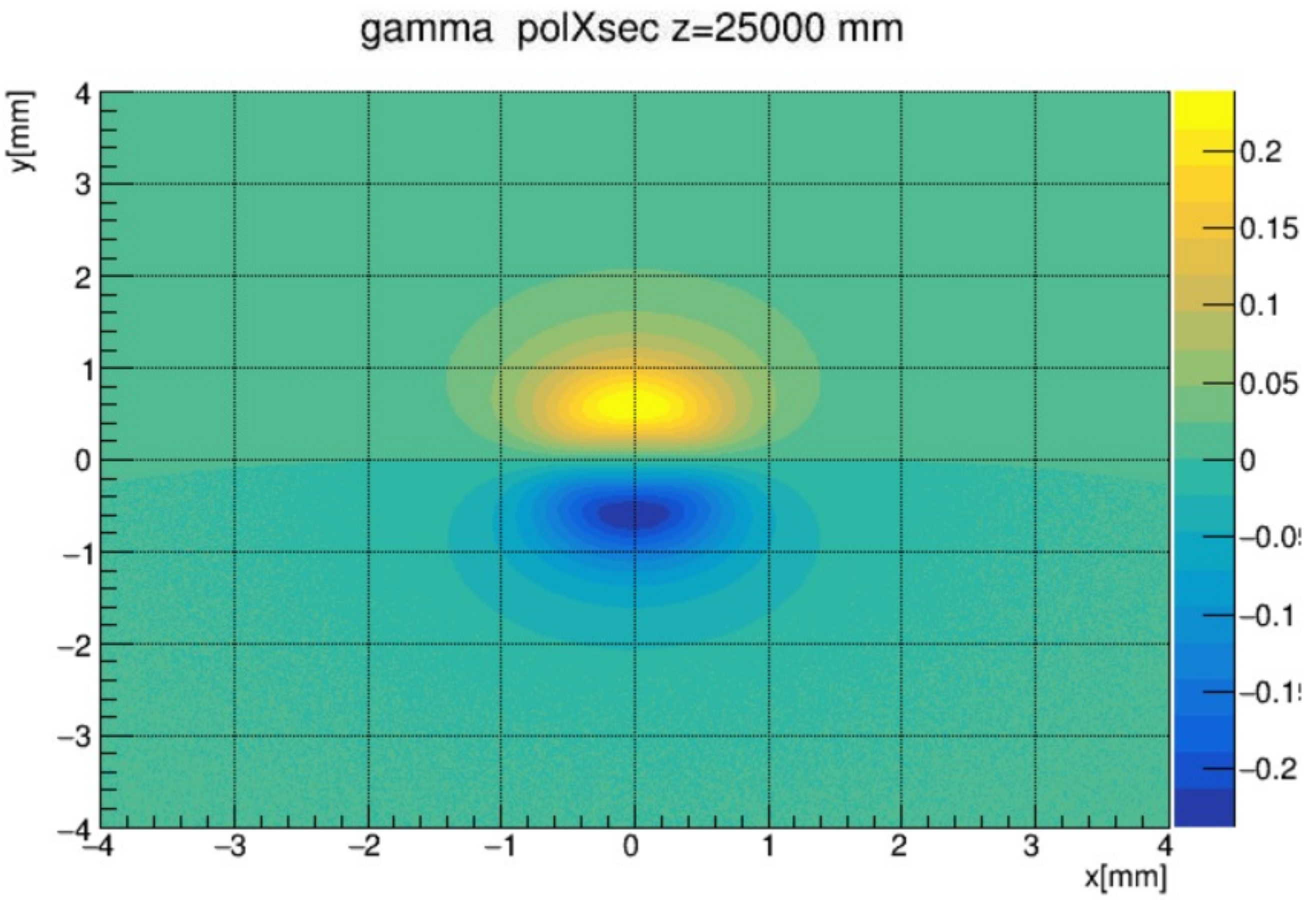

Transverse asymmetry

$$A_{\mathrm{T}} = \frac{2\pi r_o^2 a}{(d\sigma/d\rho)} \cos\phi \left[\rho(1-a)\frac{\sqrt{4a\rho(1-\rho)}}{(1-\rho(1-a))}\right]$$

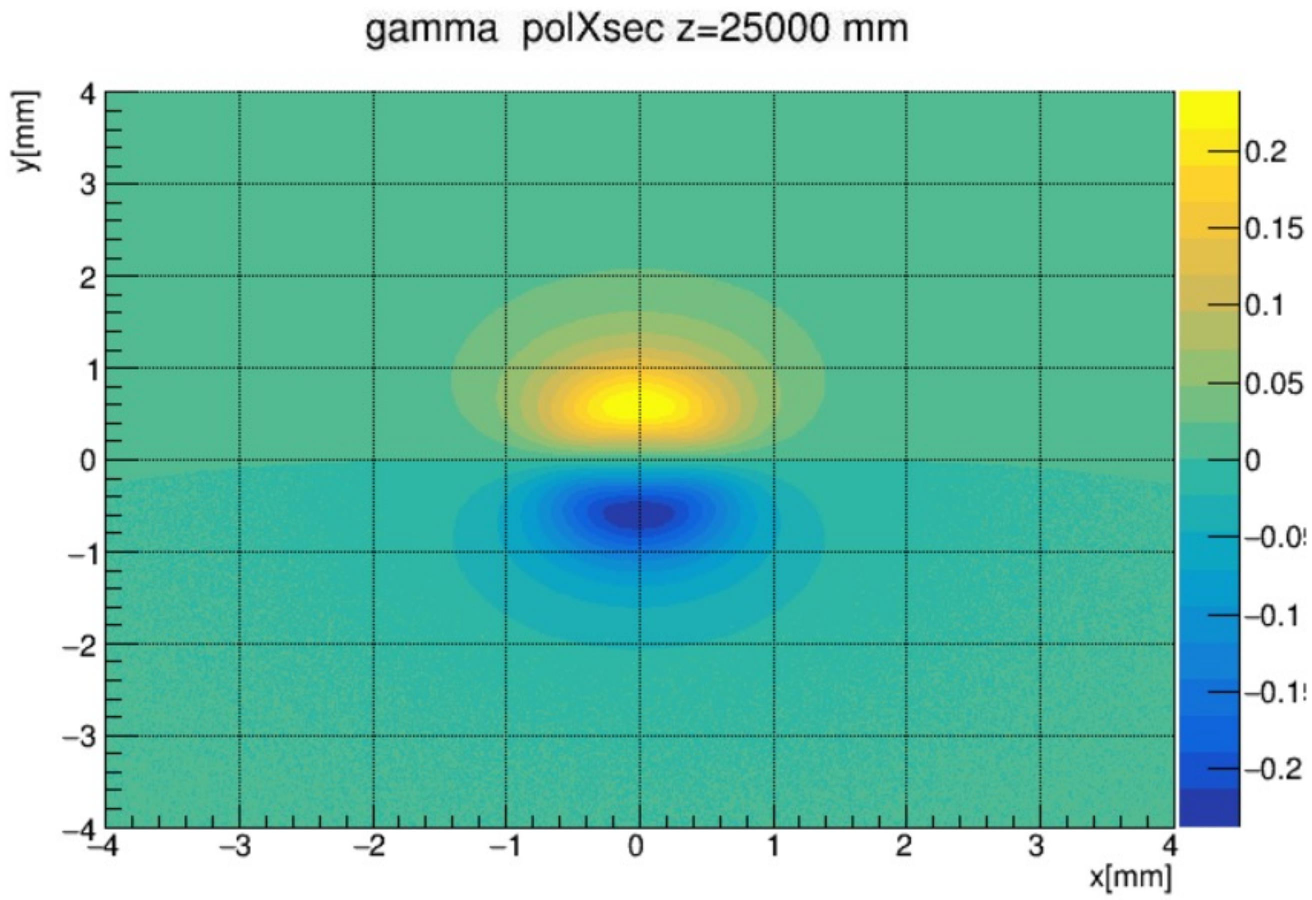

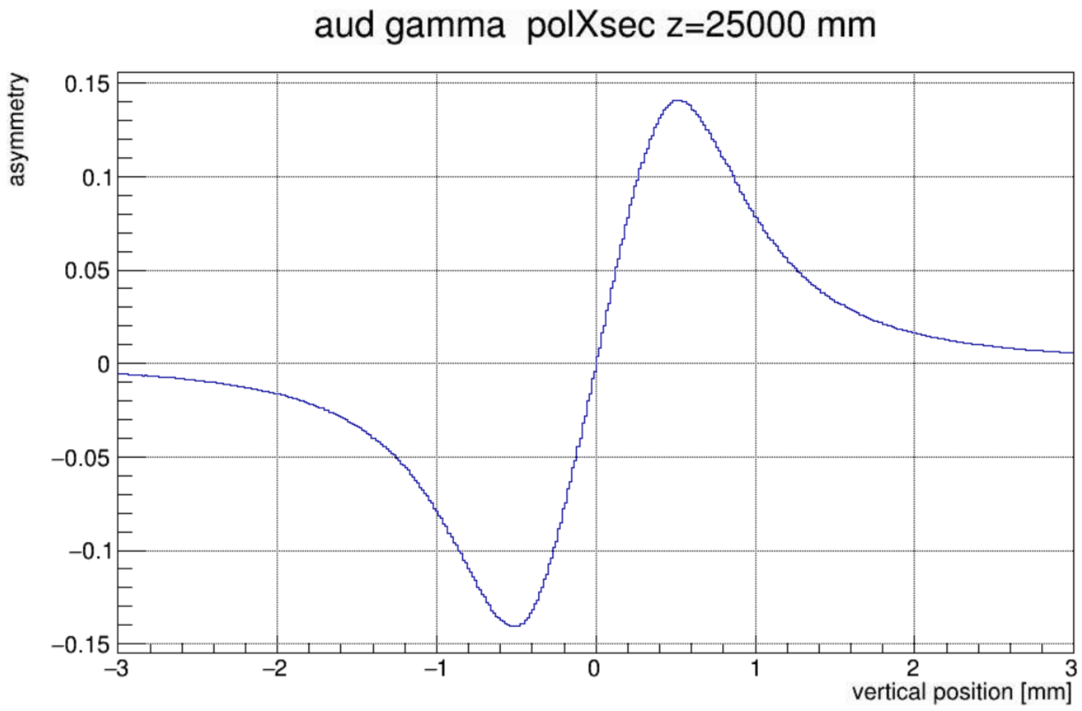

How can we make this measurement?

EIC Compton Layout

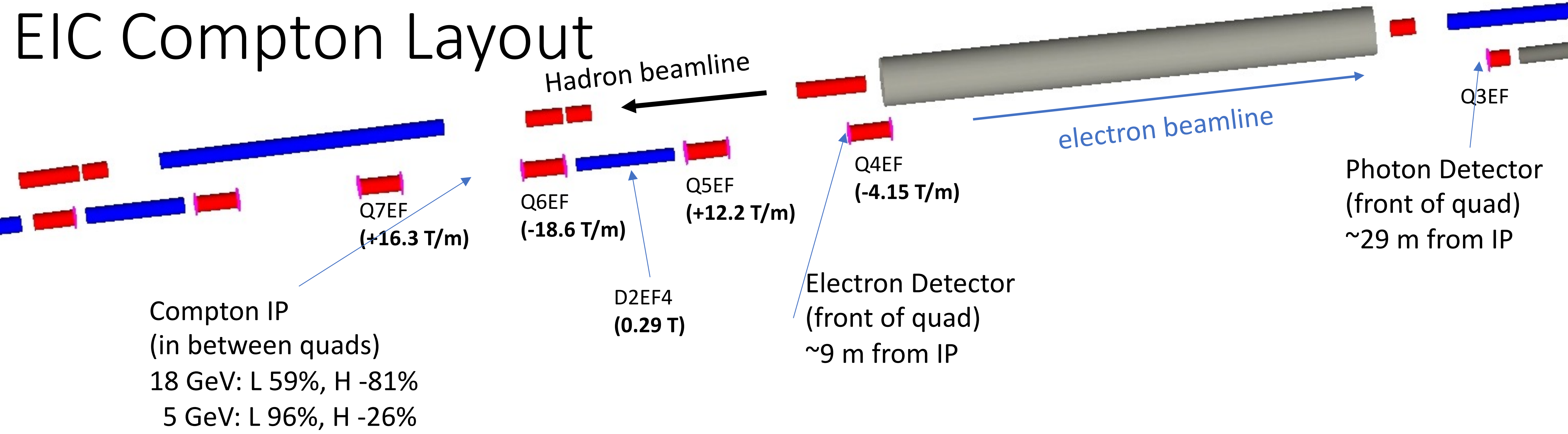

- The current configuration allows for the interaction point to be in a magnetic field free region reducing the complexity at the interaction point and allows for relatively access to insert the laser beam
- The electron detector is placed after a dipole which has enough power to energy analyze the scattered electrons at all energy set points
  - The Quad after the dipole is horizontally defocusing increasing the effectiveness of the dipole

Complex measurement

Planned Compton polarimeter location upstream of detector IP
→ Beam polarization mostly longitudinal, but some spin rotation remains before arrival at detector IP

At Compton interaction point, electrons have both longitudinal and transverse (horizontal) components
→ Longitudinal polarization measured via asymmetry as a function of backscattered photon/scattered electron energy
→ Transverse polarization from left-right asymmetry

Beam energy	P_L	P_T
5 GeV	97.6%	21.6%
10 GeV	90.7%	42.2%
18 GeV	70.8%	70.6%

Beam polarization will be fully longitudinal at detector IP, but accurate measurement of absolute polarization will require simultaneous measurement of P_L and P_T at Compton polarimeter

EIC Compton will provide first high precision measurement of P_L and P_T at the same time

Compton throughout history

Table 7. Compton polarimeters including nominal operating energies and performance. Not all Compton polarimeters are included in the table — an emphasis has been placed on those used to provide absolute beam polarization measurements.

Polarimeter	Beam energy	Laser wavelength and technology	Detection and method	Sys. uncertainty (dP/P)	References
CERN LEP	46 GeV	532 nm (pulsed)	γ/integrating	5%	99, 100
HERA LPOL	27.5 GeV	532 nm (pulsed)	γ/integrating	1.6%	85
HERA TPOL	27.5 GeV	514 nm (CW)	γ/counting	2.9%	92, 101
MIT-Bates	0.3–1 GeV	532 nm	γ/counting	6%	95, 96
NIKHEF	<1 GeV	514 nm	γ/counting	4.5% @ 440 MeV	94
Mainz A4	0.85,1.5 GeV	514 nm intra-cavity Ar–ion	(γ,e)/counting	N/A	98
JLab Hall A	1–6 GeV	1064 nm, FP cavity	γ/counting	3% (2002)	81
			e/counting	1% (2006)	102
			γ/integrating	1% (2009)	103
	1.1 GeV	532 nm, FP cavity	γ/integrating	1.1% (2010)	104, 9
JLab Hall C	1.1 GeV	532 nm, FP cavity	e/counting	0.6%	82
			γ/integrating	3%	105
SLD at SLAC	45.6 GeV	532 nm (pulsed)	e/multiphoton	0.5%	86, 106

JLab Hall A 2.1 GeV | 532nm FP cavity | photon/integrating | 0.52%

***Phys.Rev.Lett.* 129 (2022) 4, 042501

What is the problem with the Compton measurement?

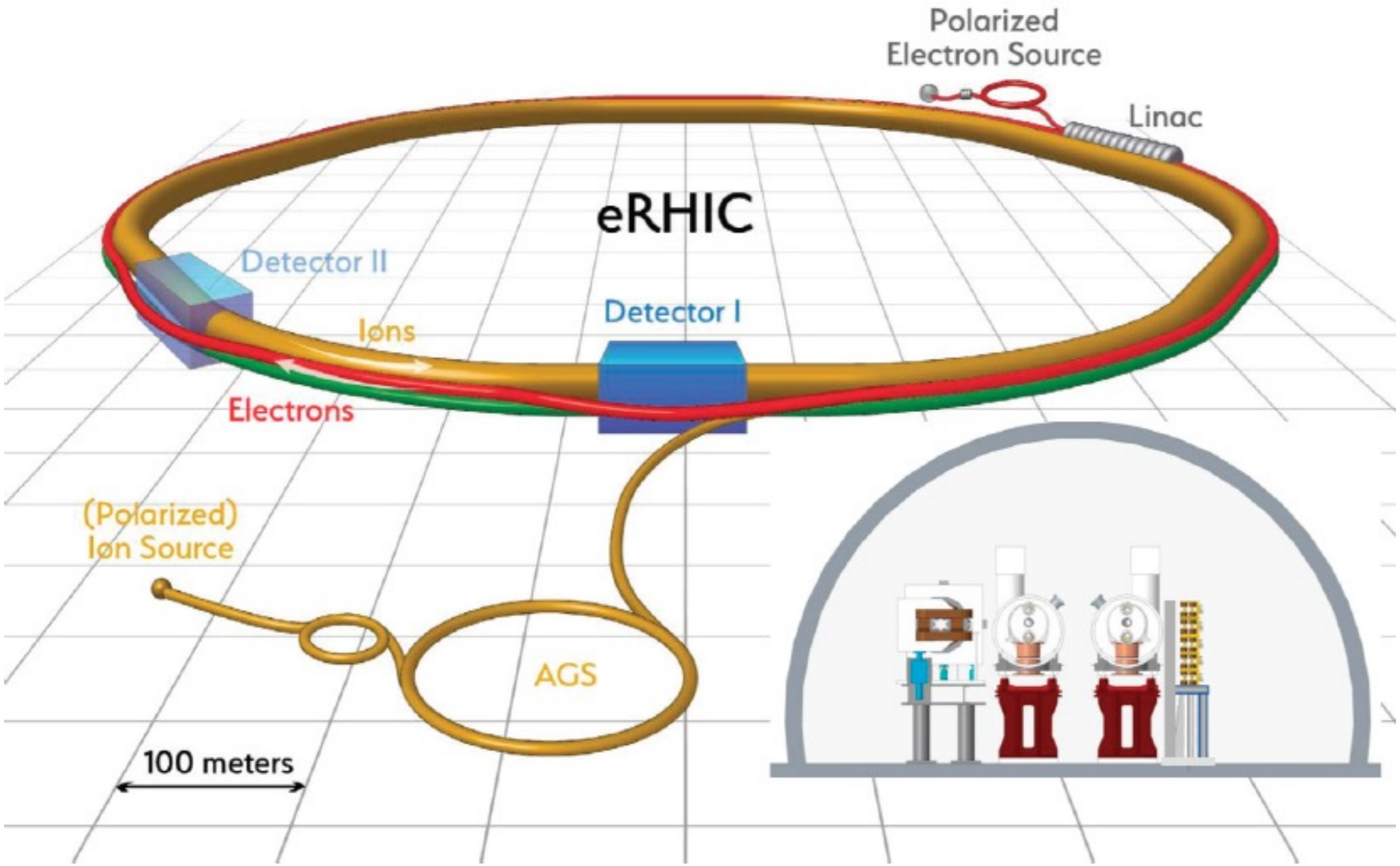

What is the problem with the Compton measurement?

- Easiest at high energies
- Non-destructive, but systematics are energy dependent

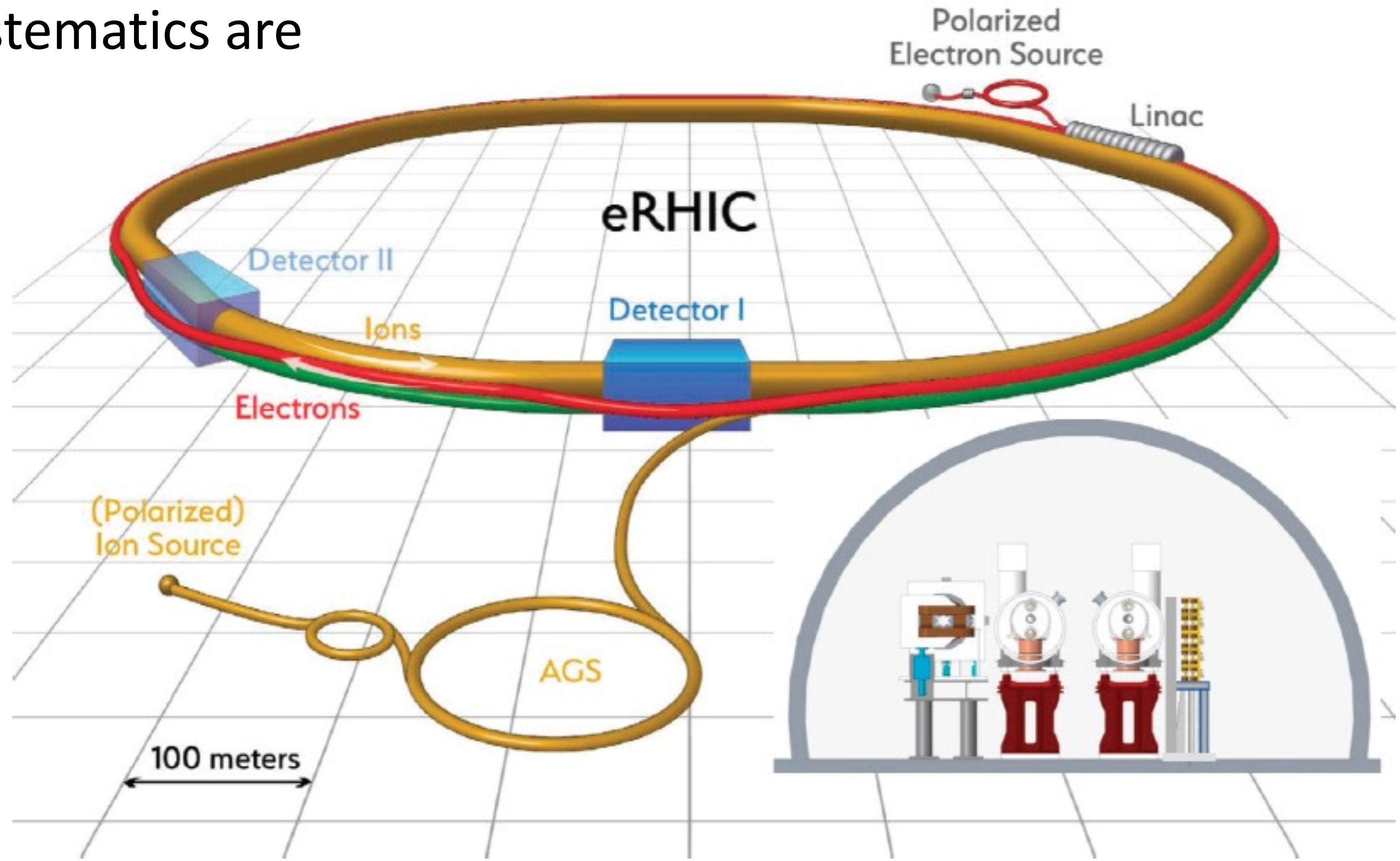

Standard electron polarimetry techniques

- Compton scattering: $\vec{e} + \vec{\gamma} \rightarrow e + \gamma$
- Mott scattering: $\vec{e} + Z \ \rightarrow e$
  - Spin-orbit coupling of electron spin with (large Z) target nucleus
  - Useful at MeV-scale (injector) energies
- Møller scattering: $\vec{e} + \vec{e} \ \rightarrow e + e$
  - Atomic electrons in Fe (or Fe-alloy) polarized using external magnetic field
  - Can be used at MeV to GeV-scale energies – rapid, precise measurements
  - Usually destructive (solid target) – non-destructive measurements possible with polarized gas target, but such measurements not common

Mott polarimetry

Mott scattering: $\vec{e} + Z \rightarrow e$

→ Spin-orbit coupling of electron spin with (large Z) target nucleus gives single-spin asymmetry for transversely polarized electrons

Mott polarimetry useful at low energies

→ ~ 100 keV to 5 MeV

→ Ideal for use in polarized electron injectors

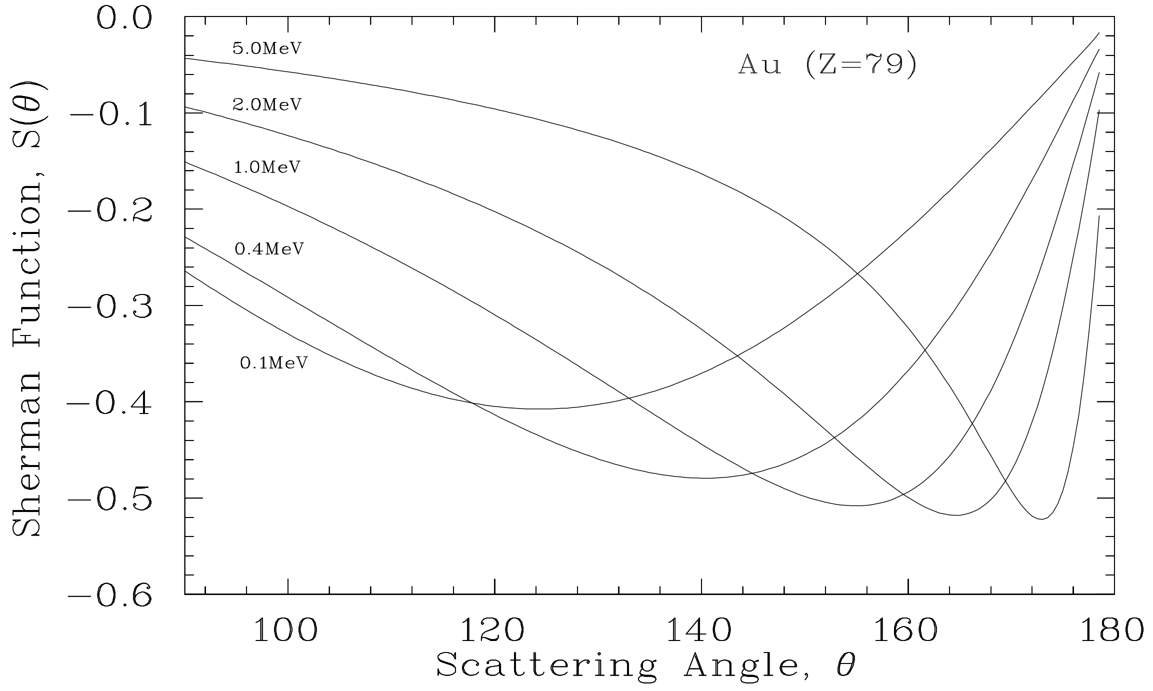

I(θ) → unpolarized cross section

$$I(\theta) = \left(\frac{Ze^2}{2mc^2}\right)^2 \frac{(1-\beta^2)(1-\beta^2\sin^2\frac{\theta}{2})}{\beta^4\sin^2\frac{\theta}{2}}$$

S(θ) is the Sherman function

→ must be calculated from electron-nucleus cross section

→ Dominant systematic uncertainty but controlled to better than 1%

Mott examples: JLab injector

- Optimized for operation at 5 MeV
  - Studied between 3-8 MeV
- Detectors at 172.7 degrees
  - Thin and thick scintillators
- Typically uses thin gold target (1 μm or less)
- Some backgrounds possible due to nearby beam dump
  - Has been studied using lower duty cycle beam + time of flight
- Recent extensive systematic studies yield overall systematic uncertainty < 1%

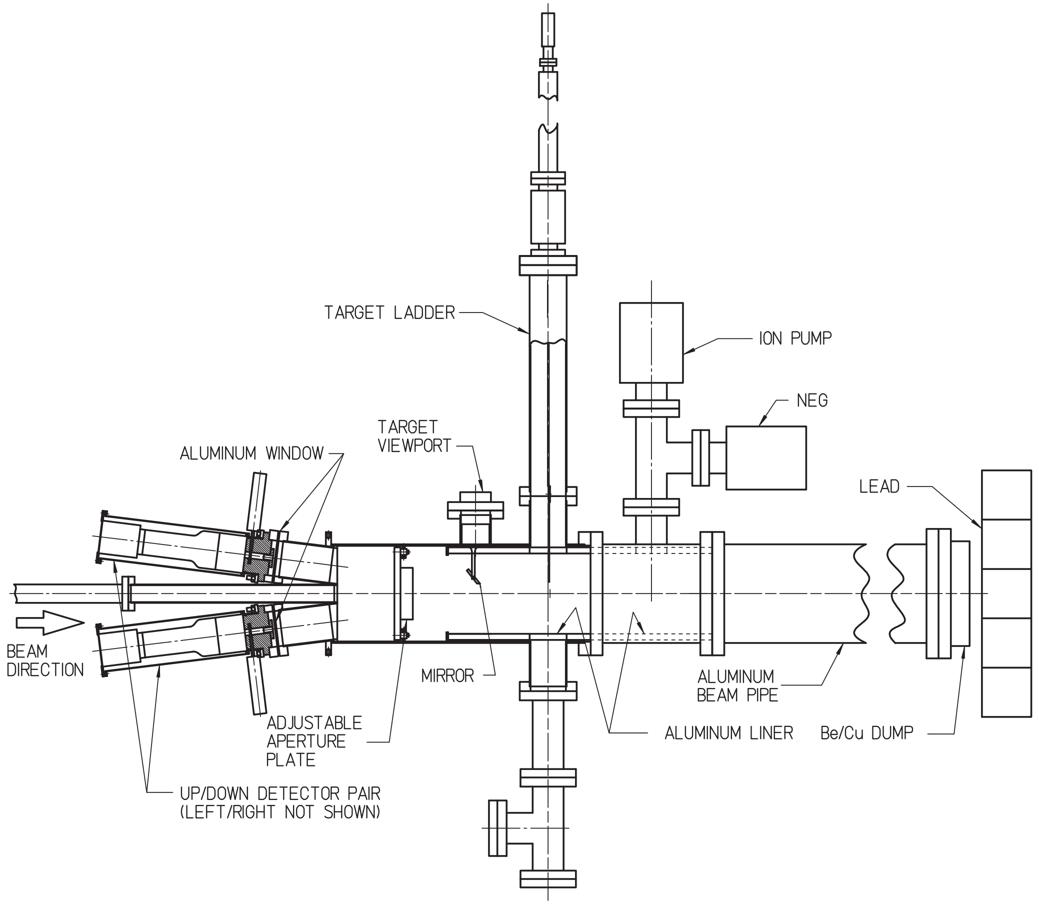

Jefferson Lab 5 MeV Mott Polarimeter

J.M. Grames et al, Phys.Rev.C 102 (2020) 1, 015501

JLab 5 MeV Mott systematics

- Much effort dedicated to demonstration of precision Mott polarimetry

→ Improved background rejection via time-of-flight cuts

→ Dedicated studies of Sherman function

→ GEANT4 simulations showed double-scattering in target foil is only source of dependence of analyzing power on target thickness

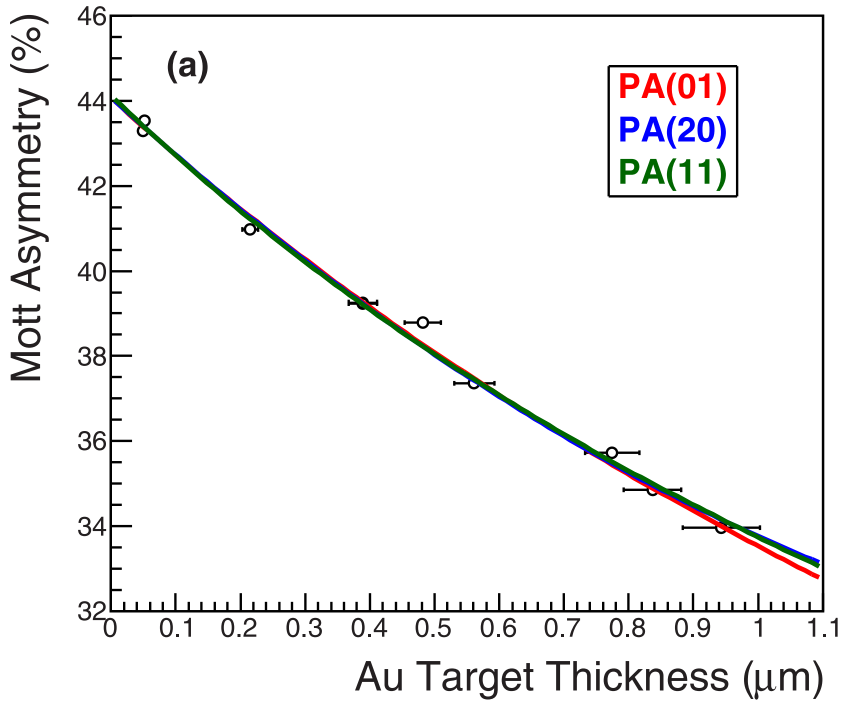

JLab 5 MeV Mott Systematic uncertainties

Contribution	Value
Sherman function	0.50%
Target thickness extrapolation	0.25%
Device-related systematics	0.24%
Energy cut (0.1%)	
Laser polarization (0.10%)	
Scattering angle/beam energy (0.20%)	
Total	**0.61%**

J.M. Grames et al, Phys.Rev.C 102 (2020) 1, 015501

Møller Scattering

$\vec{e} + \vec{e} \rightarrow e + e$

Longitudinally polarized electrons/target:

$$\frac{d\sigma}{d\Omega^*} = \frac{\alpha^2}{s}\frac{(3+\cos^2\theta^*)^2}{\sin^4\theta^*}\left[1 + P_e P_t A_{\parallel}(\theta^*)\right]$$

$$A_{\parallel} = \frac{-(7+\cos^2\theta^*)\sin^2\theta^*}{(3+\cos^2\theta^*)^2}$$

→ At θ^*=90 deg. → -7/9

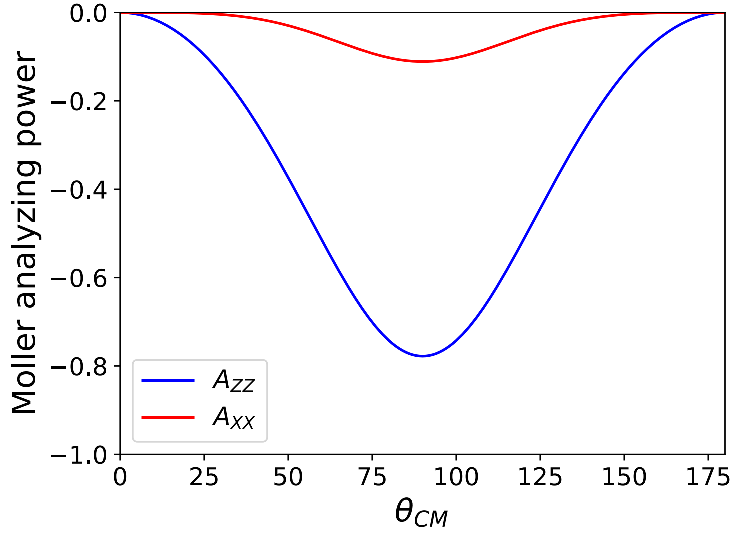

Transversely polarized electrons/target

$$A_{\perp} = \frac{-\sin^4\theta^*}{(3+\cos^2\theta^*)^2}$$

→ At θ^*=90 deg. → -1/9

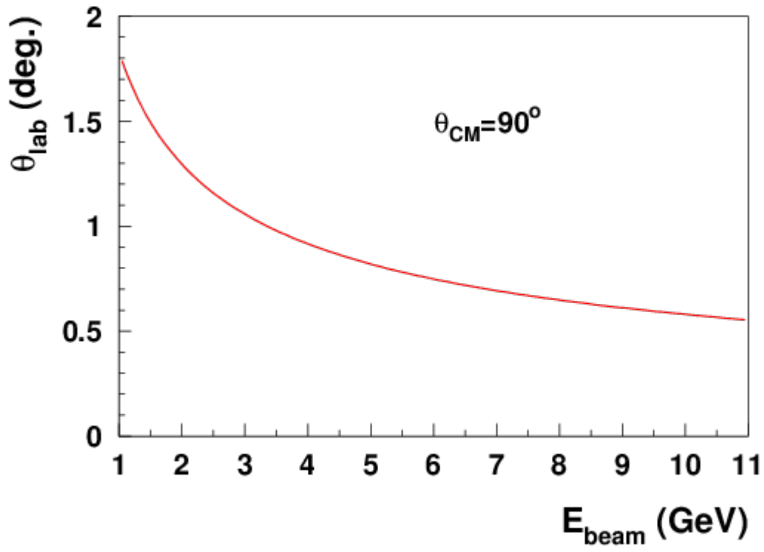

Maximum asymmetry independent of beam energy

Polarized target for Møller polarimeter

- Originally, Møller polarimeters used Fe-alloy targets, polarized in plane of the foil
  - Used modest magnetic field
- In-plane polarized targets typically result is systematic errors of 2-3%
  - Require careful measurement magnetization of foil
- Pure Fe saturated in 4 T field
  - Spin polarization well known → 0.25%
  - Temperature dependence well known
  - No need to directly measure foil polarization

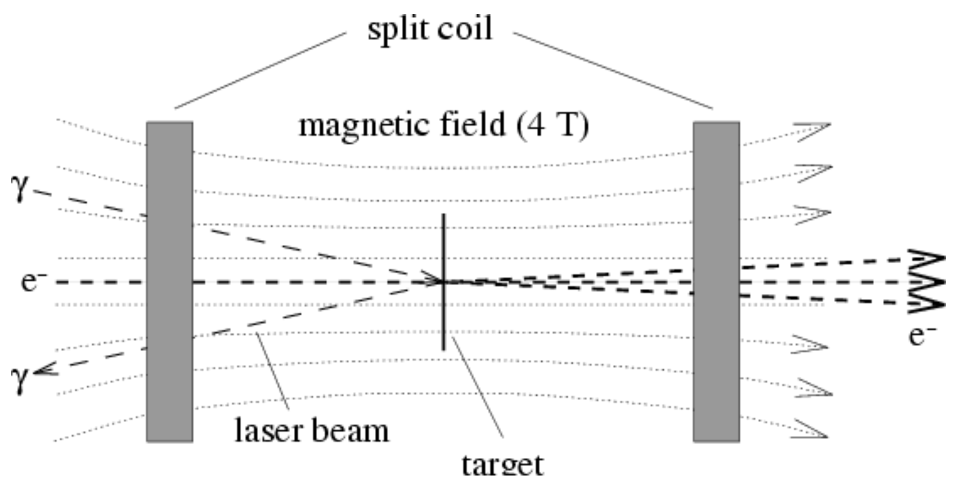

Effect	$M_s[\mu_B]$	error
Saturation magnetization (T→0 K,B→0 T)	2.2160	±0.0008
Saturation magnetization (T=294 K, B=1 T)	2.177	±0.002
Corrections for B=1→4 T	0.0059	±0.0002
Total magnetization	2.183	±0.002
Magnetization from orbital motion	0.0918	±0.0033
Magnetization from spin	2.0911	±0.004
Target electron polarization (T=294 K, B= 4 T)	0.08043	±0.00015

Foil saturation

Polarization of target not directly measured when using iron foil driven to magnetic saturation
→ Rely on knowledge of magnetic properties of iron
→ One can test that foil is in magnetic saturation using magneto-optical Kerr effect (polarization properties of light change in magnetic medium)

Can also test dependence on foil angle (misalignment) and heating

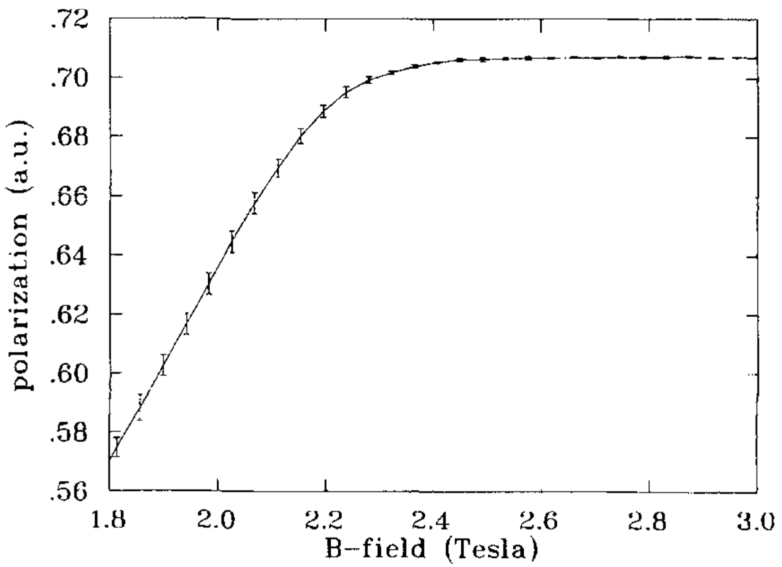

Kerr effect measurement of foil saturation

Example: Measure degree of saturation vs. applied magnetic field
→ This can also be tested with polarimeter directly

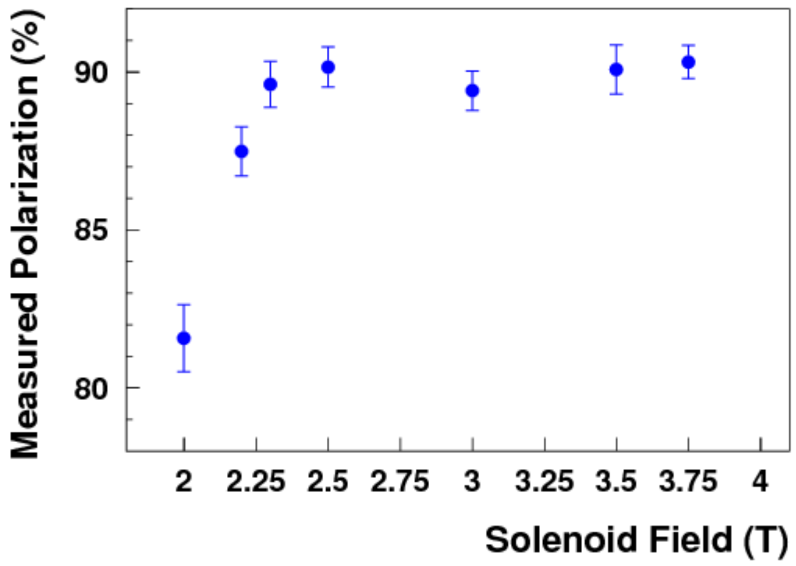

JLab measurements of asymmetry vs. applied field

Levchuk effect

- On average, about 2 out of 26 atomic electrons in Fe atom are polarized
  - Polarized electrons are in outer shells
  - Inner shell, more tightly-bound electrons are unpolarized
- Electrons scattering from inner-shell electrons result in a ”smearing” of the correlation between momentum and scattering angle
- For finite acceptance detector, this can result in lower efficiency for detection of events scattering from more tightly bound (unpolarized) electrons
- Ignoring this “Levchuk*” effect can result in incorrect polarization measurements
- First observed experimentally at SLAC in 1995 – size of effect depends on detector acceptance

**L. G. Levchuk, Nucl. Instrum. Meth. A345 (1994) 496*

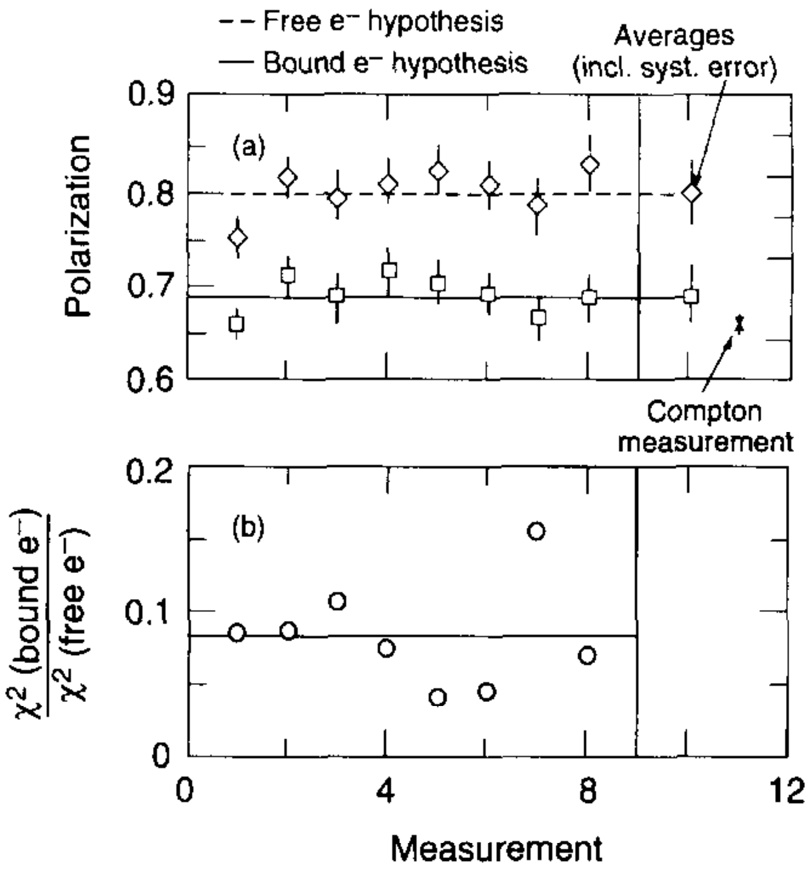

M. Swartz et al., Nucl. Instrum. Meth. A363 (1995) 526

Møller example: JLab hall C

- First polarimeter to use high field, out-of-plane polarized target
- Detects scattered and recoil electron in coincidence
- 2 quadrupole optics maintains constant tune at detector plane, independent of beam energy
- "Moderate" acceptance mitigates Levchuk effect → still a non-trivial source of uncertainty
- Target = pure Fe foil, brute-force polarized out of plane with 3-4 T superconducting magnet
- Target polarization uncertainty = ***0.25%*** *[NIM A 462 (2001) 382]*

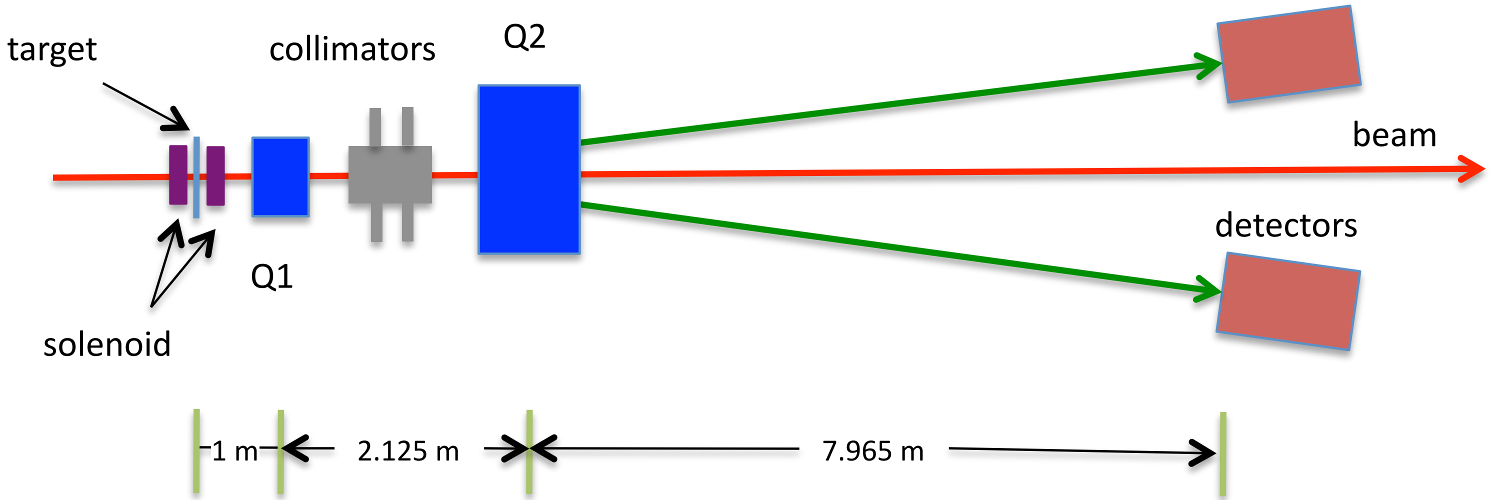

Møller examples: JLab hall C (systematics)

Source	Uncertainty	dA/A (%)
Beam position x	0.5 mm	0.17
Beam position y	0.5 mm	0.28
Beam direction x	0.5 mr	0.10
Beam direction y	0.5 mr	0.10
Q1 current	2% (1.9 A)	0.07
Q3 current	2.5% (3.25 A)	0.05
Q3 position	1 mm	0.10
Multiple scattering	10%	0.01
Levchuk effect	10%	0.33
Collimator positions	0.5 mm	0.03
Target temperature	100%	0.14
B-field direction	2^o	0.14
B-field strength	5%	0.03
Spin polarization in Fe		0.25
Electronic D.T.	100%	0.04
Solenoid focusing	100%	0.21
Solenoid position (x,y)	0.5 mm	0.23
Additional point–to–point		0.0
High current extrapolation		0.5
Monte Carlo statistics		0.14
Total		0.85

Systematic error table from Q-Weak (2nd run) in Hall C (2012)

→ Some uncertainties larger than usual due to low beam energy (1 GeV)

→ Levchuk effect, target polarization same at all energies

Total uncertainty less than 1%

Compton example: JLab Hall A

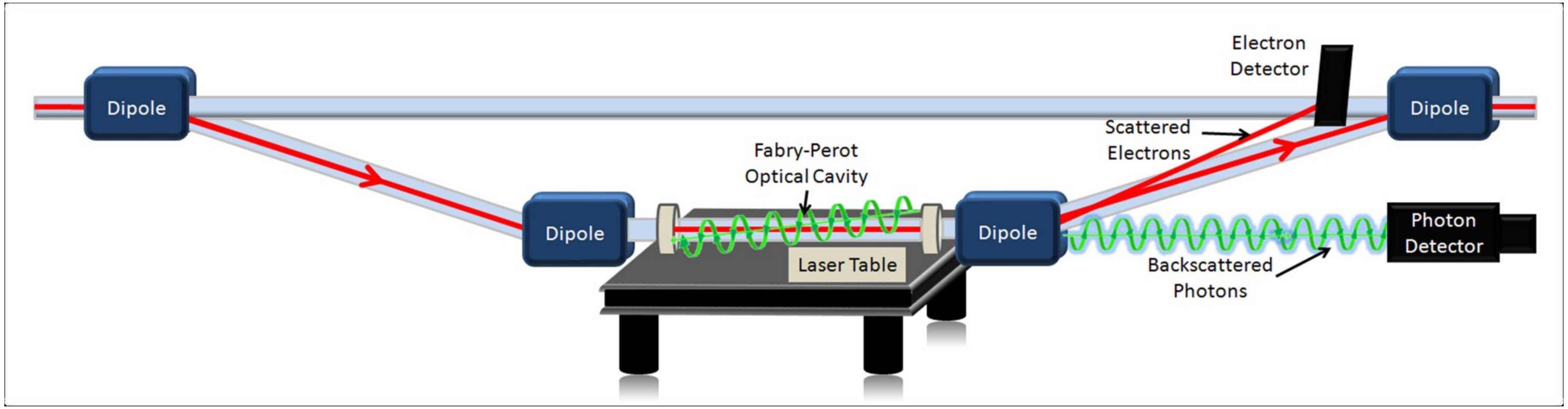

Compton polarimeter in Hall A (similar design in Hall C):

1. 4 dipole chicane to deflect beam to laser system
2. Fabry-Perot cavity to provide kW level CW laser power
3. Diamond/silicon strip detectors for scattered electrons
4. Photon detectors operated in integrating mode

→ Hall A has achieved dP/P=0.52% (photon detection)

Recap

$$A_{\parallel} = \frac{1}{P_e P_h}\left[\frac{N^{++} - RN^{+-}}{N^{++} + RN^{+-}}\right]$$

$$A_{\text{measured}} = P_{\text{beam}} A_{\text{effective}}$$

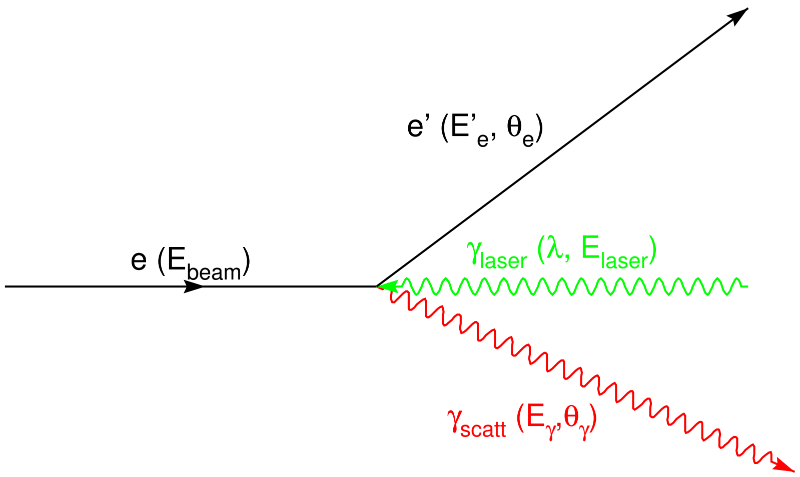

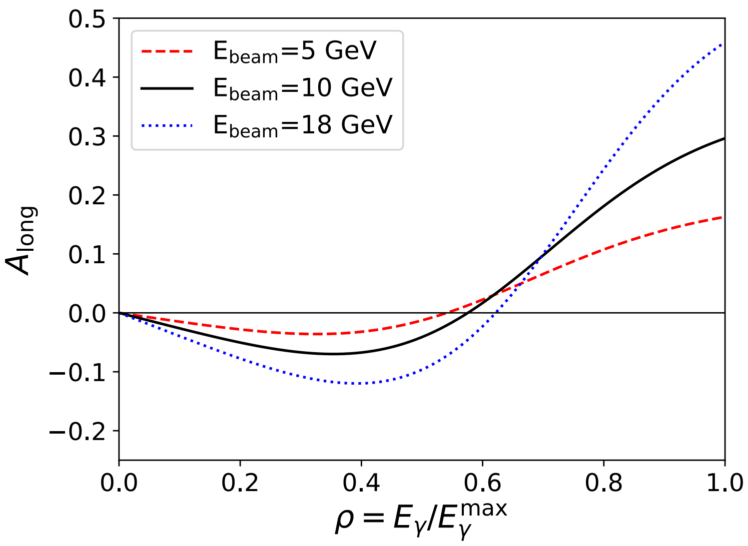

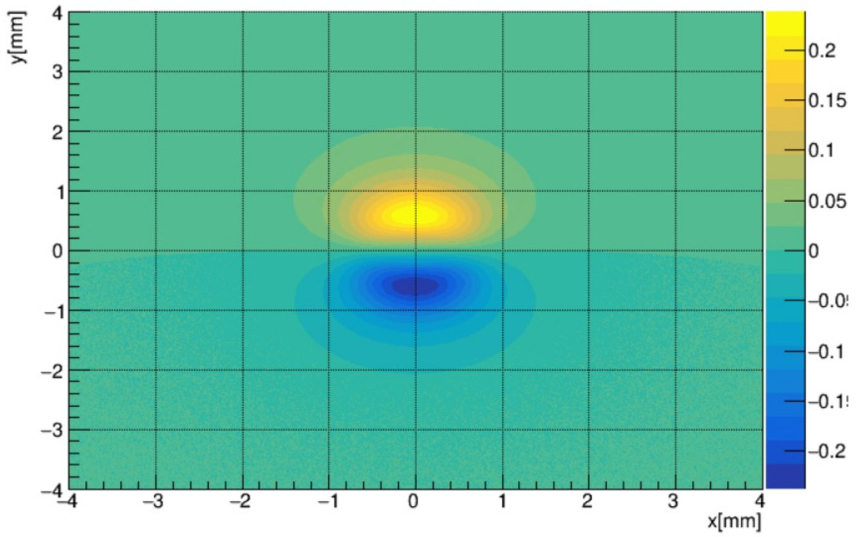

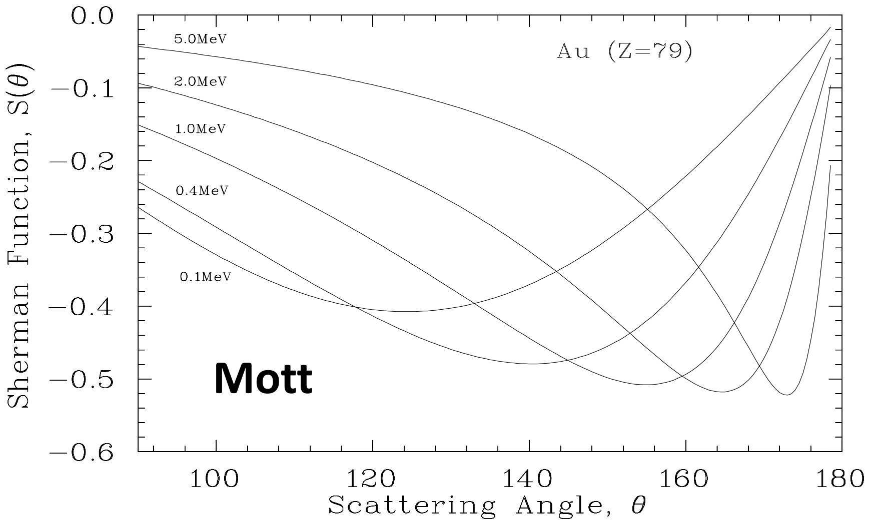

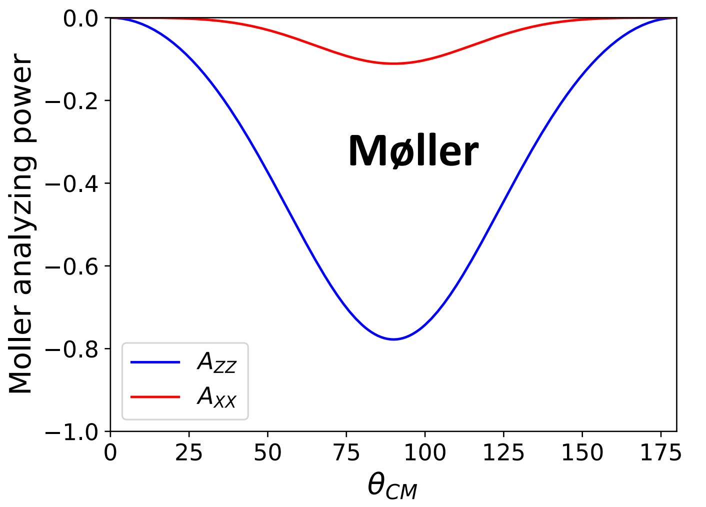

What polarimetry systematic is reasonable for the EIC?

Backups

A-trans for 1, 5, 18 GeV (532 nm)

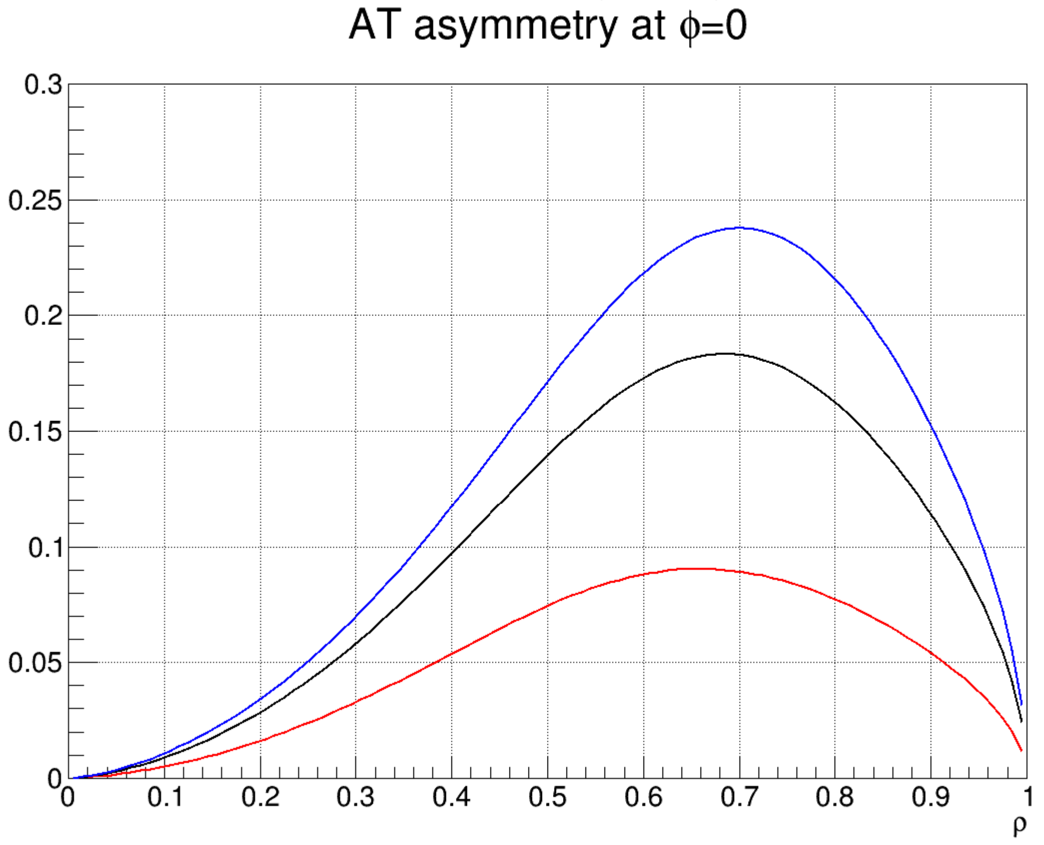

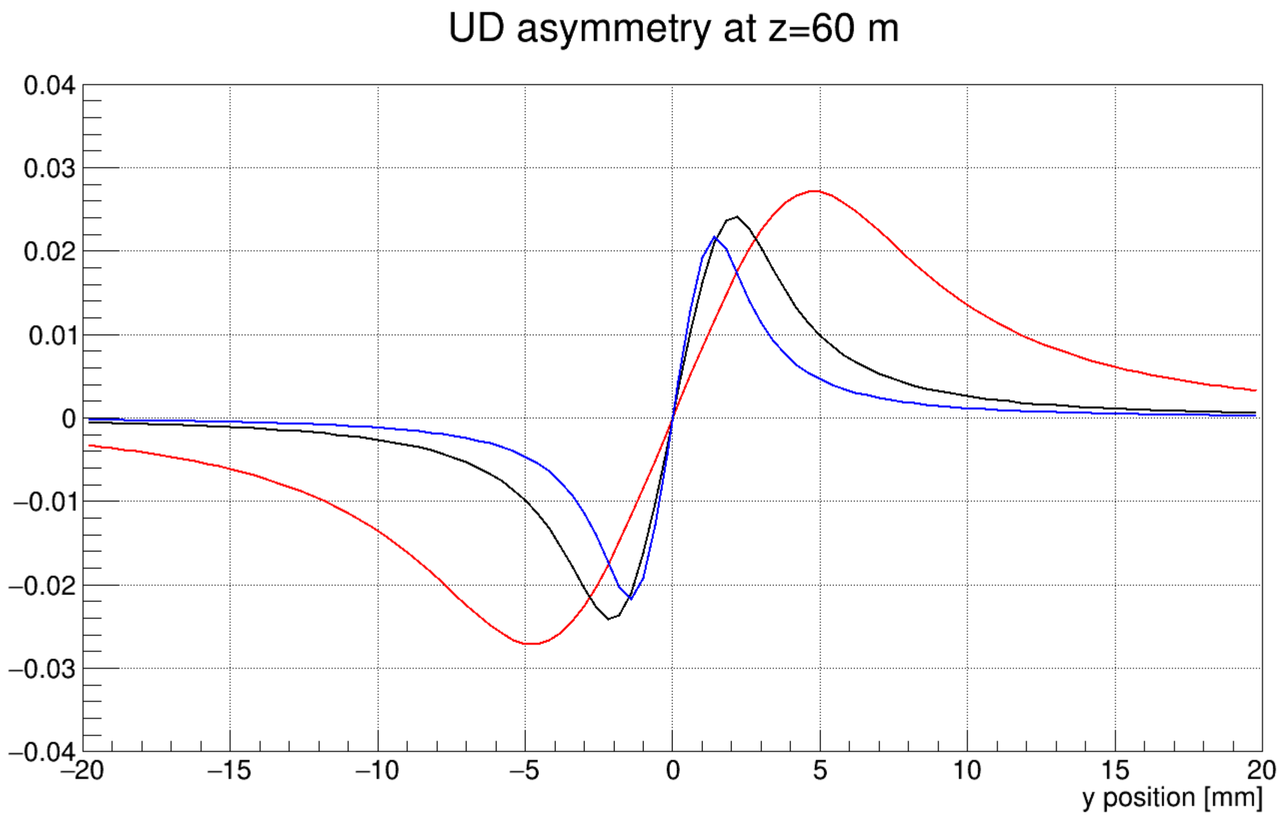

$$A_{\mathrm{T}} = \frac{2\pi r_o^2 a}{(d\sigma/d\rho)} \cos\phi \left[\rho(1-a)\frac{\sqrt{4a\rho(1-\rho)}}{(1-\rho(1-a))}\right]$$

HERA LPOL

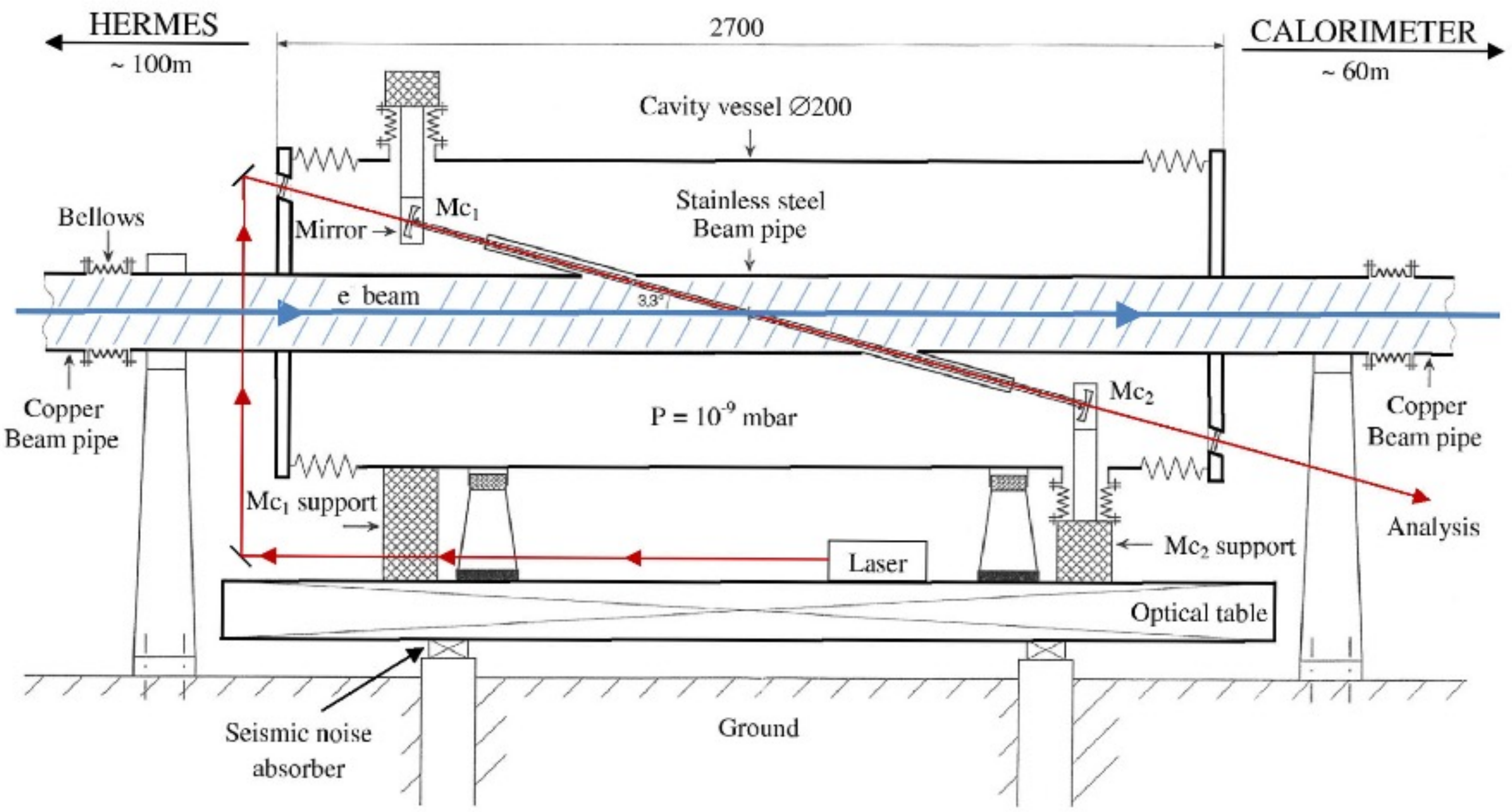

Figure 1. Scheme of the cavity surrounding the electron beam pipe with the laser and main mirrors.

- Crossing angle 3.3 deg (58mrad)
- Single photon mode: ngamma= 0.001 per crossing; s/b=0.2; 1%msmt at 2.5h
- Multiphoton mode: ngamma=1000; pulsed laser 100Hz (HERA 10MHz); 1% 1min

Sherman function

Sherman function describes single-atom elastic scattering from atomic nucleus

$$S(\theta) = i\frac{fg^* - gf^*}{f^2 + g^2}$$

Direct amplitude

Spin flip amplitude

f and *g* can be calculated exactly for spherically symmetric charge distribution

Knowledge of nuclear charge distribution and atomic electron distribution leads to systematic error
→ Controlled better than 0.5% for regime 2-10 MeV

In target with finite thickness, electron may scatter more than once → Effective Sherman function
→ Controlled by making measurements at various foil thicknesses and extrapolating to zero

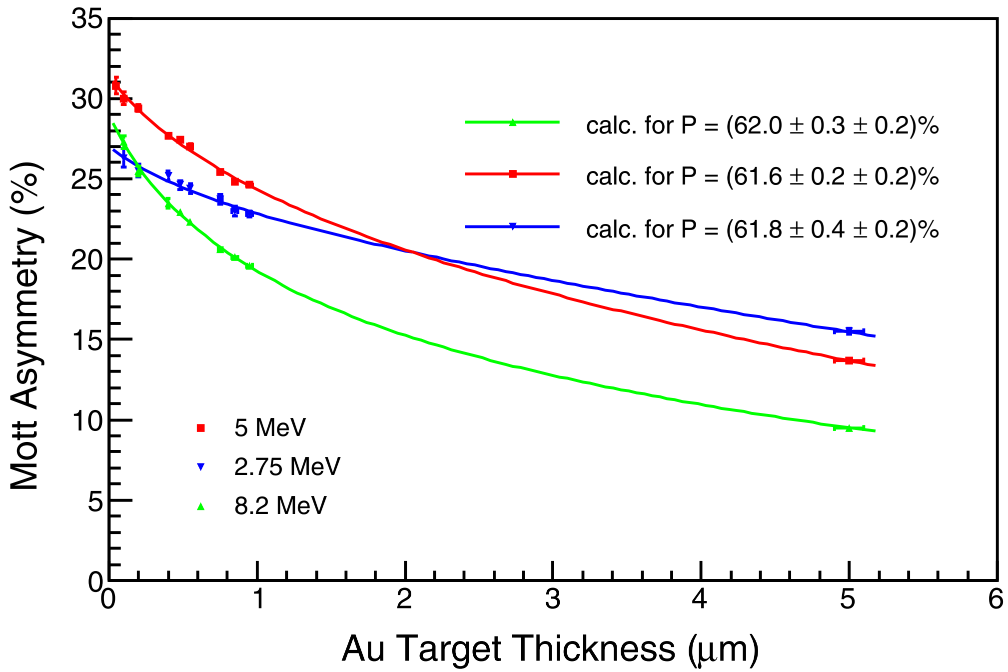

Mott examples: MAINZ MeV

Mott polarimeter in MAMI accelerator at Mainz installed after injector linac

Scattering angle = 164 degrees
→ Sherman function peaks at 2 MeV

Background from dump suppressed by using deflection magnets to steer scattered electrons to detectors – no direct line of site to beam dump

Dominant systematics from Sherman function, zero-thickness extrapolation, background
→ GEANT simulations suggest backgrounds ~ 1%

Systematic uncertainty better than 1% achievable with some additional effort

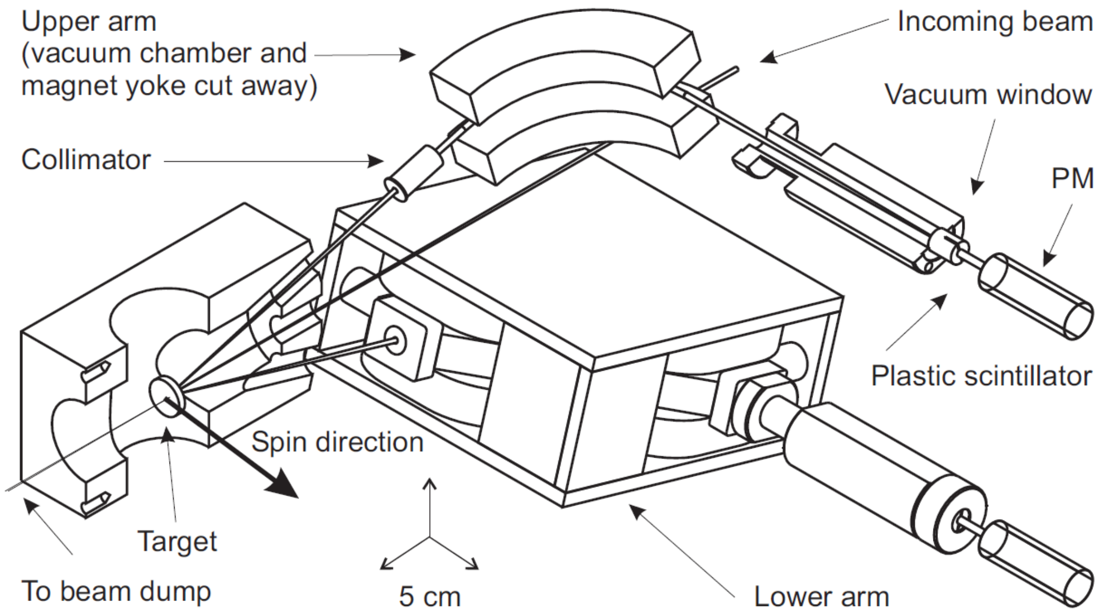

Double-Mott polarimeter

Use double-scattering to measure effective Sherman function empirically

→ Unpolarized electrons scatter from target foil – resulting polarization: $P_{scatt} = S_{eff}$
→ Polarized electrons scatter from 2nd, ***identical*** foil

Resulting asymmetry : $A_{obs} = S^2_{eff}$

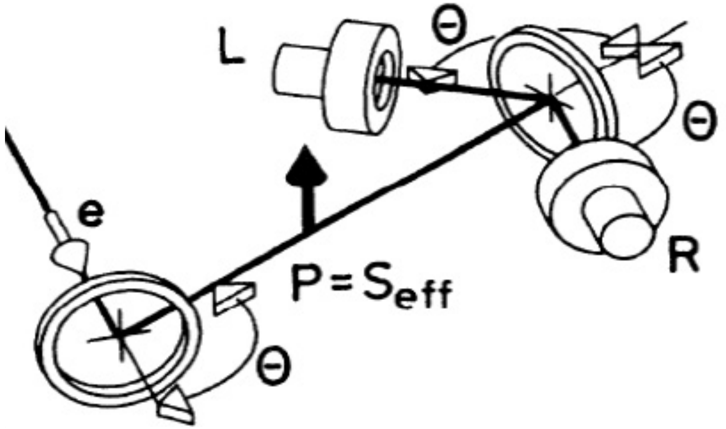

Møller polarimetry

- Møller polarimetry benefits from large longitudinal analyzing power → -7/9 (transverse → -1/9)
  → Asymmetry independent of energy
  → Relatively slowly varying near $\vartheta_{cm}=90^o$
  → Large asymmetry diluted by need to use iron foils to create polarized electrons
- Large boost results in Møller events near $\theta_{cm}=90^o$ having small lab angle
  → Magnets/spectrometer required so that detectors can be adequate distance from beam
- Dominant backgrounds from Mott scattering – totally suppressed via coincidence detection of scattered and recoiling electrons
- Rates are large, so rapid measurements are easy
- The need to use Fe or Fe-alloy foils means measurement must be destructive
- Foil depolarization at high currents

$$\vec{e} + \vec{e} \rightarrow e + e$$

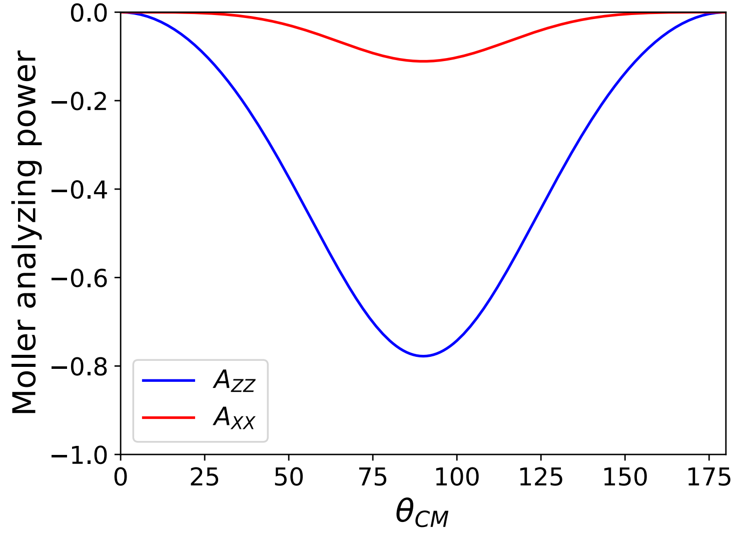

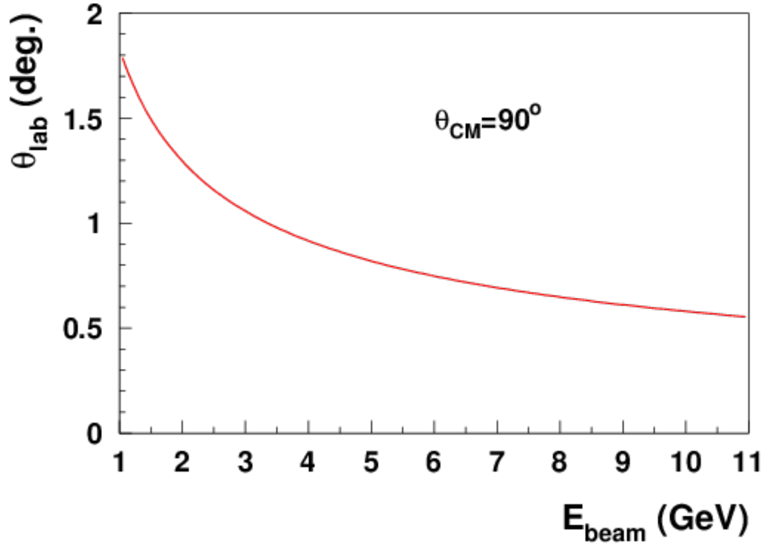

Polarized target for Møller polarimeter

- Originally, Møller polarimeters used Fe-alloy targets, polarized in plane of the foil
  - Used modest magnetic field
- In-plane polarized targets typically result is systematic errors of 2-3%
  - Require careful measurement magnetization of foil
- Pure Fe saturated in 4 T field
  - Spin polarization well known → 0.25%
  - Temperature dependence well known
  - No need to directly measure foil polarization

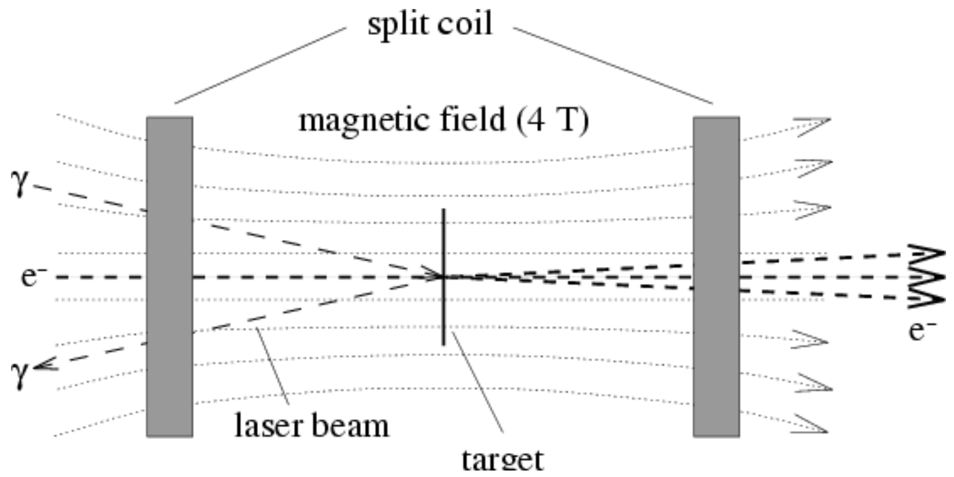

Effect	$M_s[\mu_B]$	error
Saturation magnetization (T→0 K,B→0 T)	2.2160	±0.0008
Saturation magnetization (T=294 K, B=1 T)	2.177	±0.002
Corrections for B=1→4 T	0.0059	±0.0002
Total magnetization	2.183	±0.002
Magnetization from orbital motion	0.0918	±0.0033
Magnetization from spin	2.0911	±0.004
Target electron polarization (T=294 K, B= 4 T)	0.08043	±0.00015

Foil saturation

Polarization of target not directly measured when using iron foil driven to magnetic saturation
→ Rely on knowledge of magnetic properties of iron
→ One can test that foil is in magnetic saturation using magneto-optical Kerr effect (polarization properties of light change in magnetic medium)

Can also test dependence on foil angle (misalignment) and heating

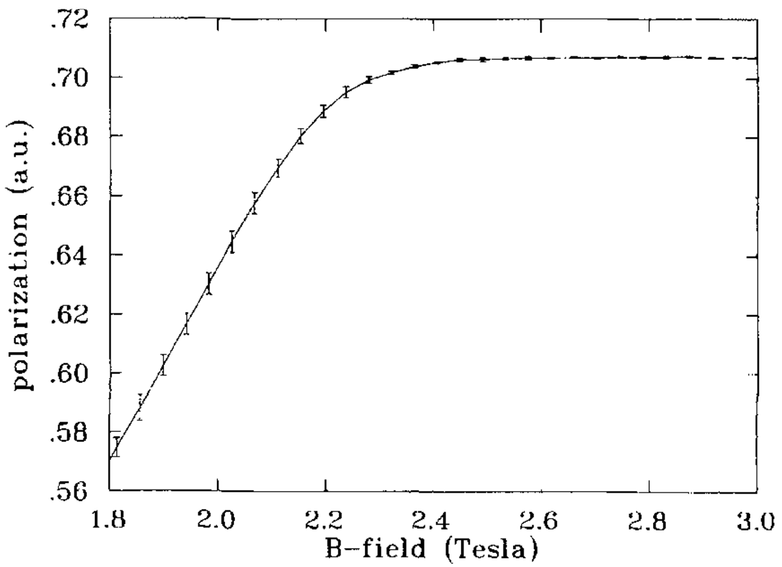

Kerr effect measurement of foil saturation

Example: Measure degree of saturation vs. applied magnetic field
→ This can also be tested with polarimeter directly

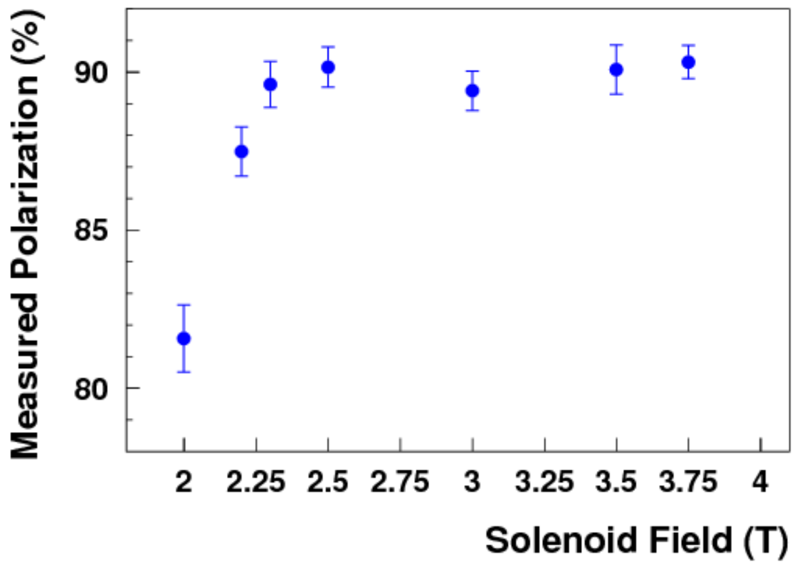

JLab measurements of asymmetry vs. applied field

Levchuk effect

- On average, about 2 out of 26 atomic electrons in Fe atom are polarized
  - Polarized electrons are in outer shells
  - Inner shell, more tightly-bound electrons are unpolarized
- Electrons scattering from inner-shell electrons result in a ”smearing” of the correlation between momentum and scattering angle
- For finite acceptance detector, this can result in lower efficiency for detection of events scattering from more tightly bound (unpolarized) electrons
- Ignoring this “Levchuk*” effect can result in incorrect polarization measurements
- First observed experimentally at SLAC in 1995 – size of effect depends on detector acceptance

*L. G. Levchuk, Nucl. Instrum. Meth. A345 (1994) 496

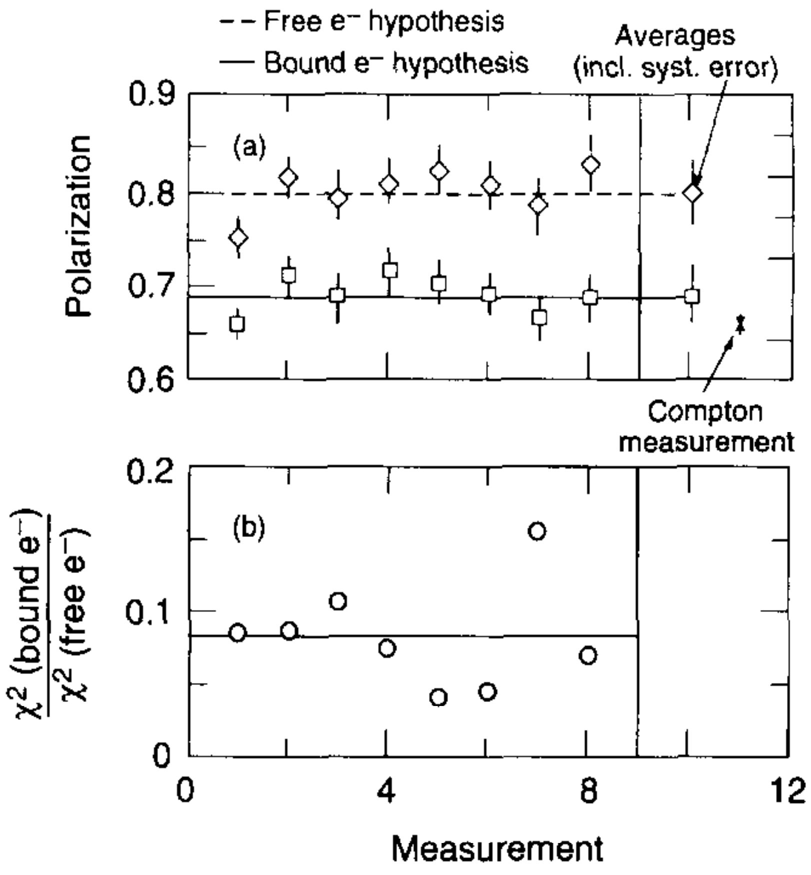

M. Swartz et al., Nucl. Instrum. Meth. A363 (1995) 526

Møller example: SLAC E154

Single-arm polarimeter used in End Station at SLAC in the 1990's

- → Low field, in-plane polarized target
- → 2-detectors, but did not detect scattered and recoil electrons in coincidence
- → Scattered electrons steered to detectors using dipole – no focusing quads
- → Electrons detected with silicon strip detectors
- → Overall systematic uncertainty 2.4%, dominated by target polarization (1.7%) and background subtraction (2%)

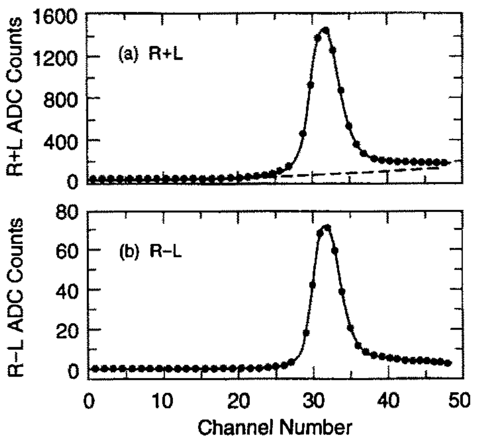

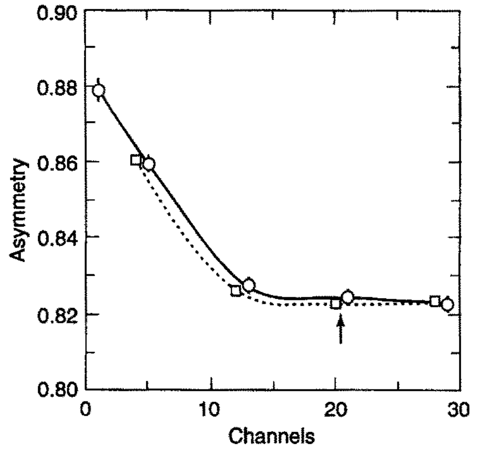

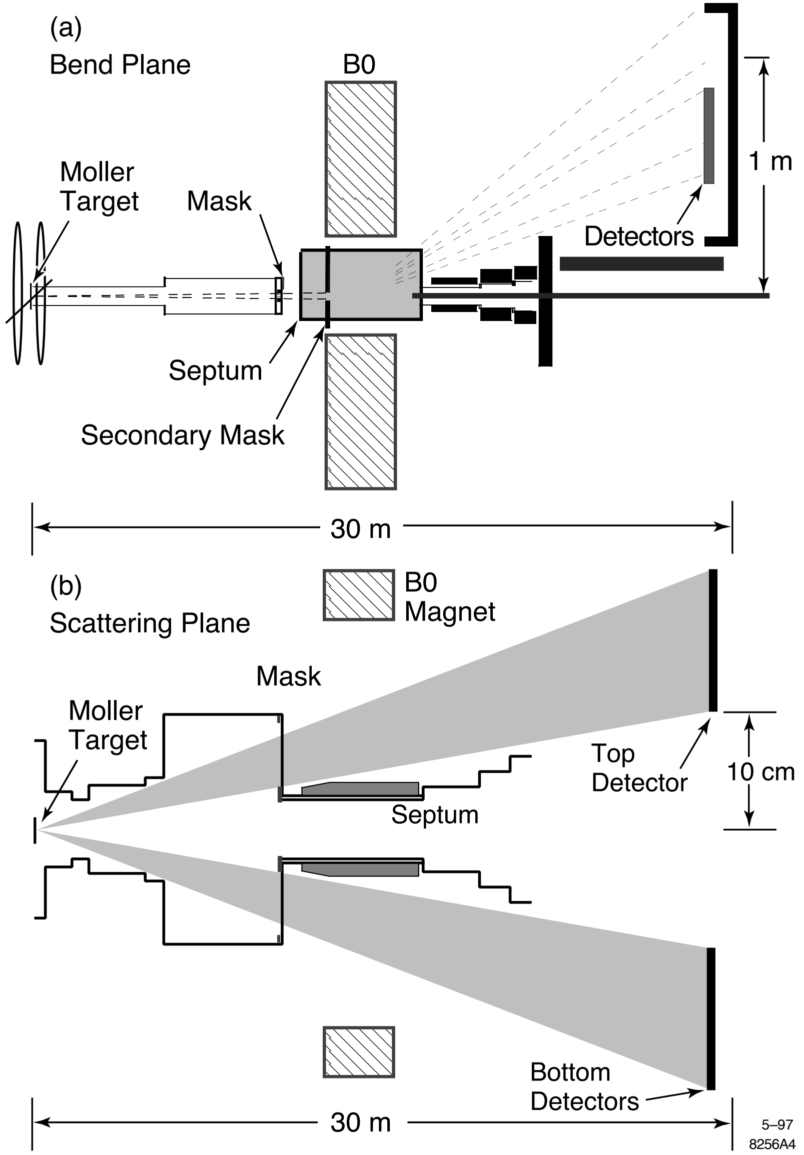

Møller example: JLab hall C

- First polarimeter to use high field, out-of-plane polarized target
- Detects scattered and recoil electron in coincidence
- 2 quadrupole optics maintains constant tune at detector plane, independent of beam energy
- "Moderate" acceptance mitigates Levchuk effect → still a non-trivial source of uncertainty
- Target = pure Fe foil, brute-force polarized out of plane with 3-4 T superconducting magnet
- Target polarization uncertainty = ***0.25%*** *[NIM A 462 (2001) 382]*

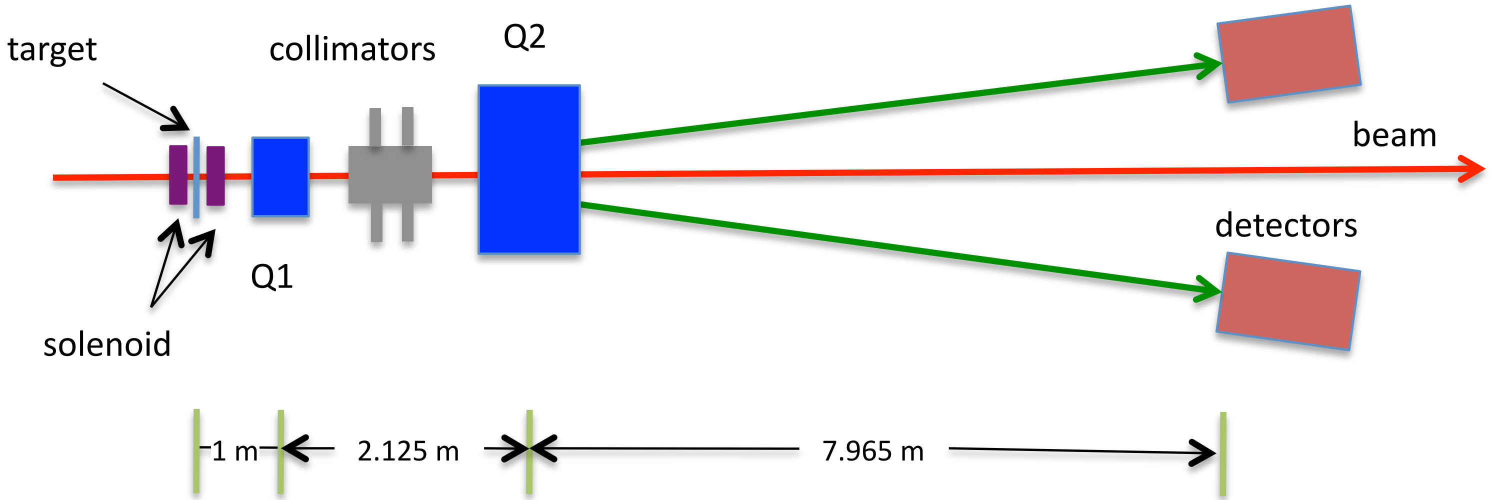

Møller examples: JLab hall C (systematics)

Source	Uncertainty	dA/A (%)
Beam position x	0.5 mm	0.17
Beam position y	0.5 mm	0.28
Beam direction x	0.5 mr	0.10
Beam direction y	0.5 mr	0.10
Q1 current	2% (1.9 A)	0.07
Q3 current	2.5% (3.25 A)	0.05
Q3 position	1 mm	0.10
Multiple scattering	10%	0.01
Levchuk effect	10%	0.33
Collimator positions	0.5 mm	0.03
Target temperature	100%	0.14
B-field direction	2^o	0.14
B-field strength	5%	0.03
Spin polarization in Fe		0.25
Electronic D.T.	100%	0.04
Solenoid focusing	100%	0.21
Solenoid position (x,y)	0.5 mm	0.23
Additional point–to–point		0.0
High current extrapolation		0.5
Monte Carlo statistics		0.14
Total		0.85

Systematic error table from Q-Weak (2nd run) in Hall C (2012)

→ Some uncertainties larger than usual due to low beam energy (1 GeV)

→ Levchuk effect, target polarization same at all energies

Total uncertainty less than 1%

Møller polarimetry with atomic hydrogen

Proposal to use atomic hydrogen as target; operates at full beam current, non-destructive measurement

→at 300 mK, 8 T, P_e ~ 100%

→density ~ 3 10^{15} cm^{-3}

→lifetime >1 hour

→Expected precision < 0.5%!

Contamination, depolarization expected to be small → < 10^{-4}

Such a target allows measurements concurrent with running experiment, mitigates Levchuk effect

System is under development for use at MAINZ for the P2 experiment → polarization measurements expected within the next couple years

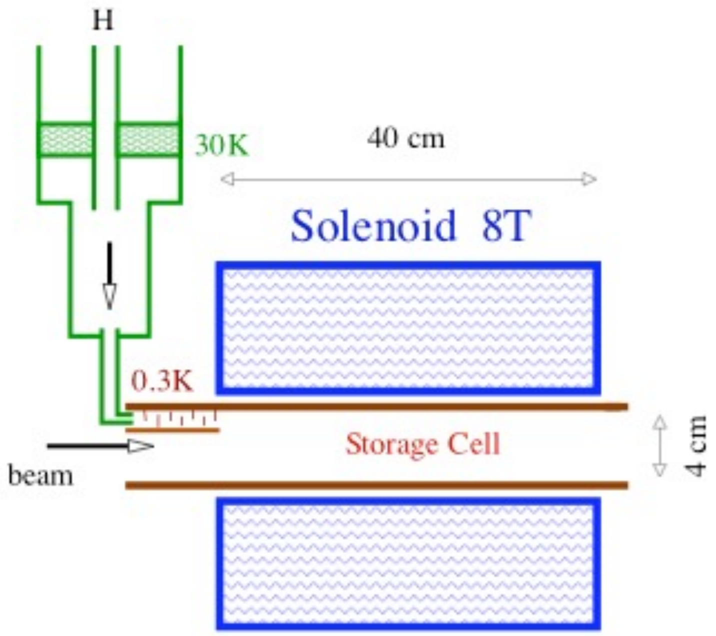

Application at EIC?

→ Gas heating by radiation drops density by factor ~ 100 to 1000

→Beam creates field 0.2-2 kV/cm – traps positive ions

Maybe some kind of H jet target can be used instead?

Møller polarimetry with jet targets

- Møller not typically used in storage rings since commonly used targets are destructive to the beam → iron and iron-alloy foils

→Jet target would be non-destructive – some measurements with jet targets have been done at VEPP-3

- What precision on target polarization can be achieved with jet targets?

→RHIC H-JET target polarization known to better than 1%

- Some R&D would be required, but precision Møller polarimetry in storage rings may be feasible

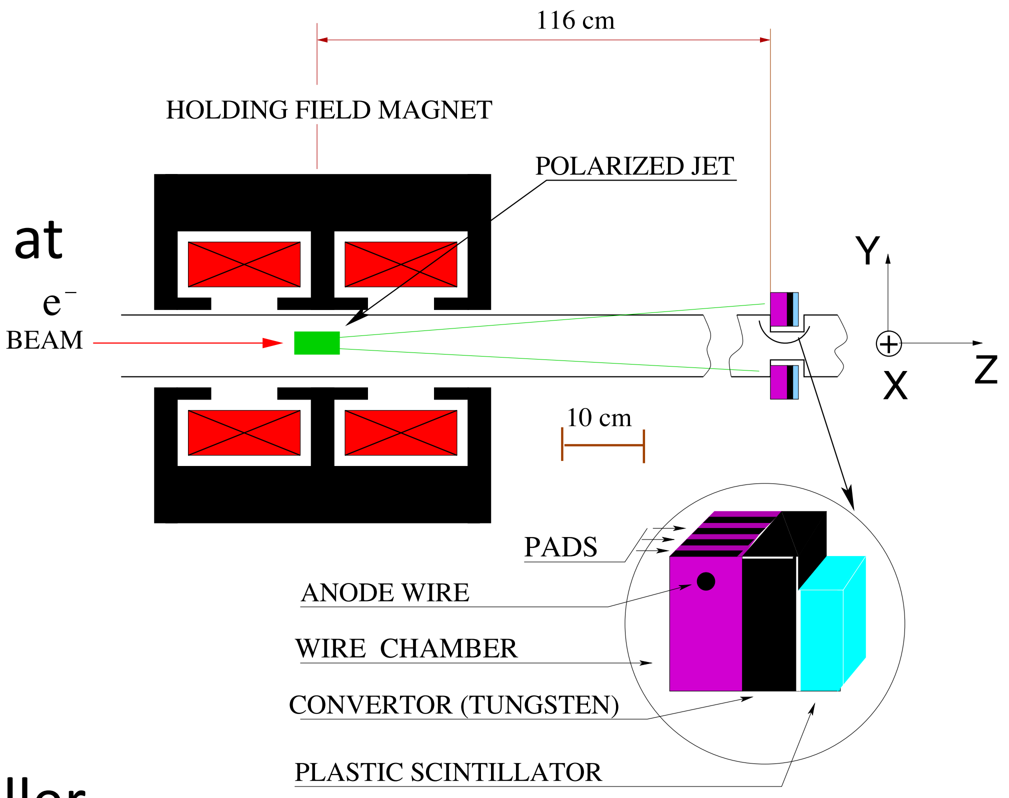

A. Grigoriev et al, Proceedings of EPAC 2004

Compton example: JLab Hall A

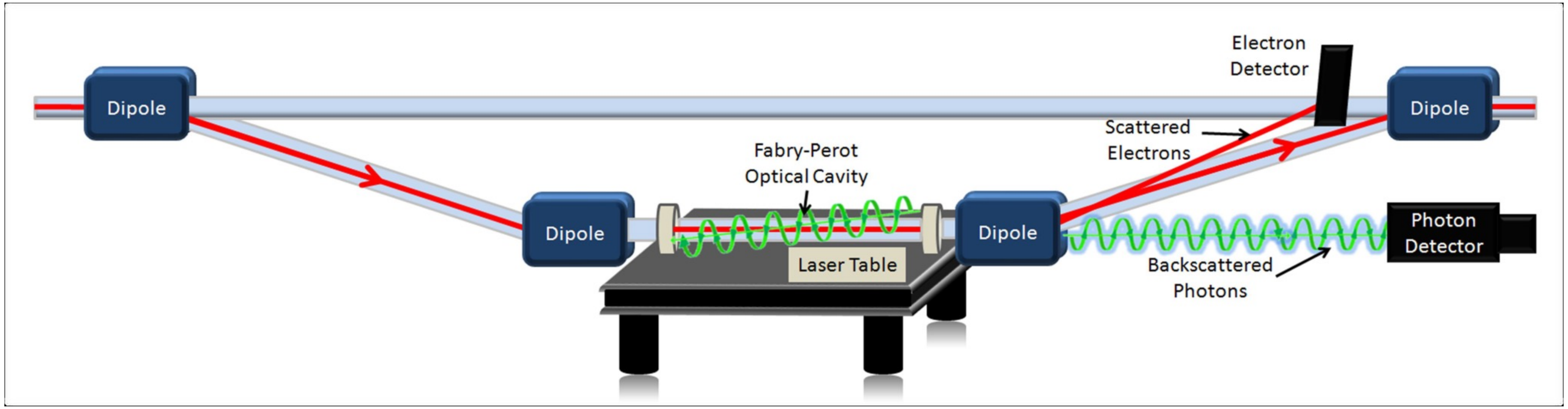

Compton polarimeter in Hall A (similar design in Hall C):

1. 4 dipole chicane to deflect beam to laser system
2. Fabry-Perot cavity to provide kW level CW laser power
3. Diamond/silicon strip detectors for scattered electrons
4. Photon detectors operated in integrating mode

→ Hall A has achieved dP/P=0.52% (photon detection)

Fabry-Perot Cavity Laser System

Due to relatively low intensity of JLab electron beam, need higher laser power

→ Use external Fabry-Perot cavity to amplify 1-10 W laser to 1-5 kW of stored laser power

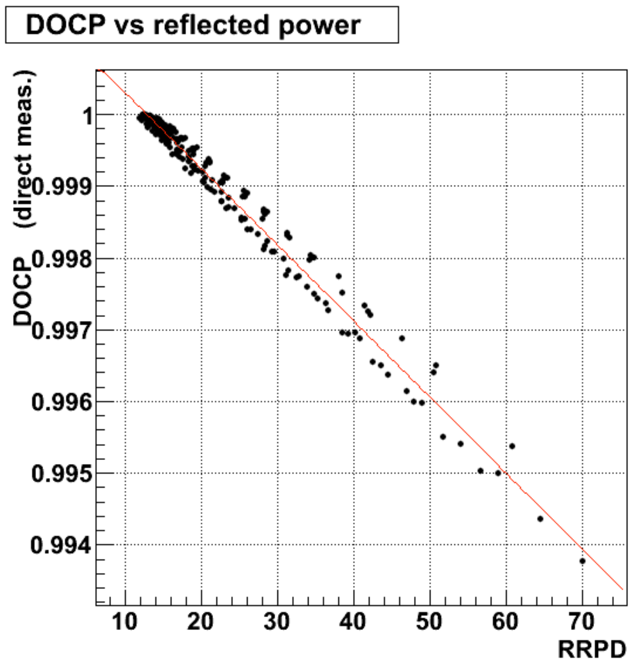

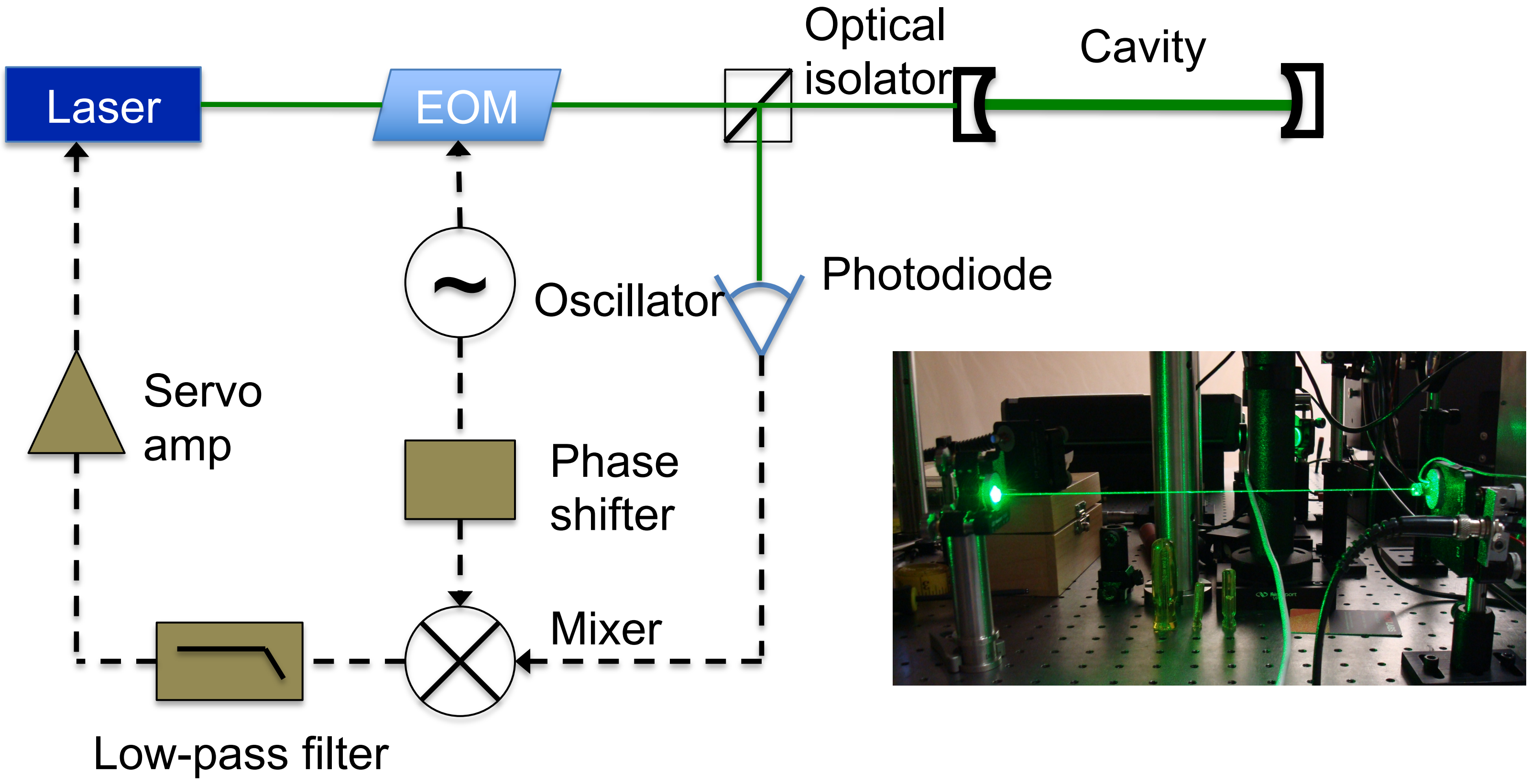

Key systematic: Laser polarization in Fabry-Perot cavity

→ Constrain by monitoring light reflected back from cavity and measurement of cavity birefringence

Compton photon detector

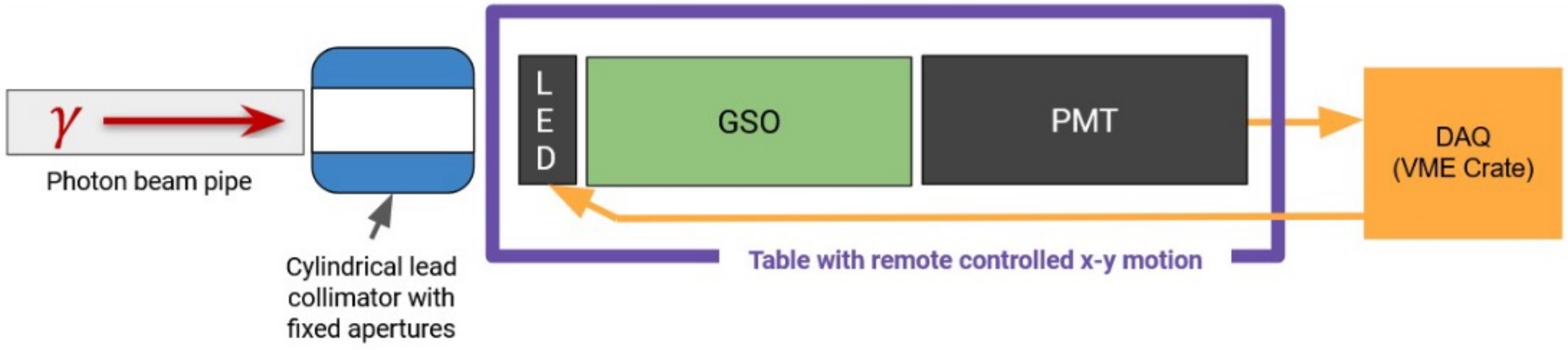

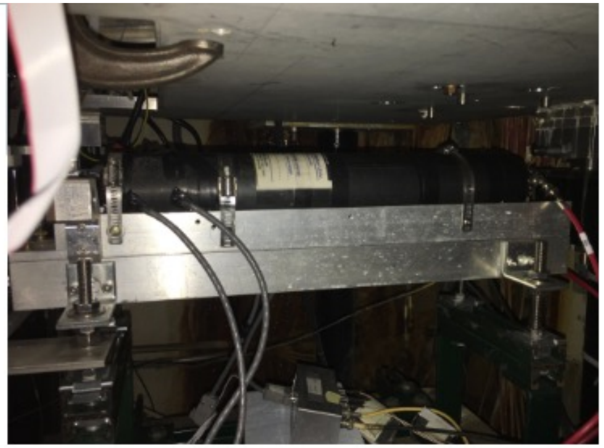

- Detector Components
  - Pb Collimator
  - GSO Scintillator
  - PMT and DAQ readout
- Signals integrated over helicity state
- Measure helicity-correlated asymmetry
- LED's allow for in situ detector tests

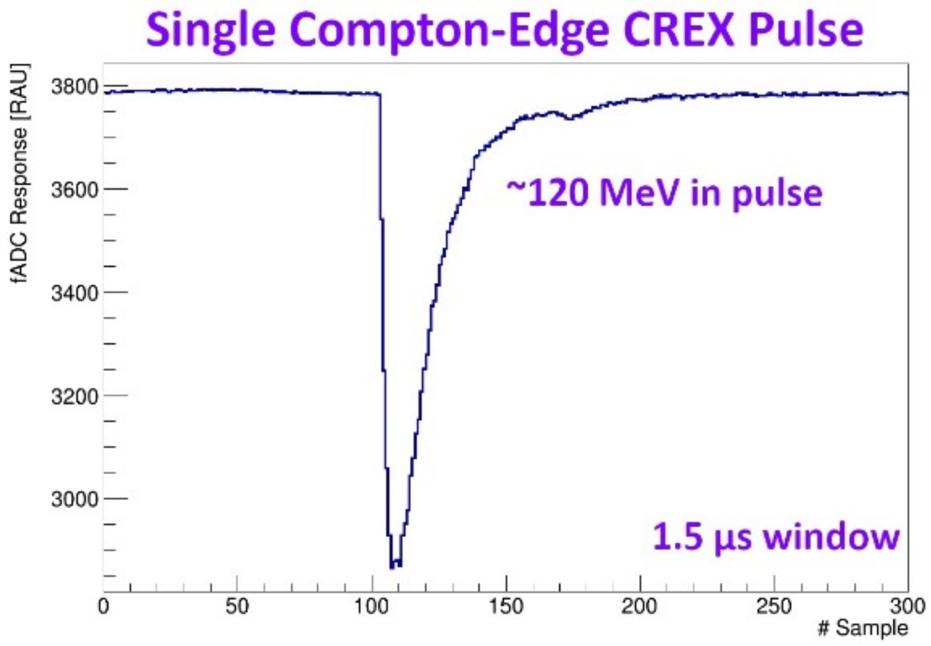

A. Zec Thesis: DOI: [10.18130/xpq1-7090](https://doi.org/10.18130/xpq1-7090)

How the sausage is made

How to measure a Compton Asymmetry: Integrate the signal over pedestal per helicity state.
Measure signal S, for each laser state ON, OFF and helicity state $+,-$.
Helicity pattern difference (Δ), sum (Y), and asymmetry ($\mathcal{A}$) distributions are calculated:

$$\Delta_{ON} = S^+_{ON} - S^-_{ON}$$
$$\Delta_{OFF} = S^+_{OFF} - S^-_{OFF}$$
$$Y_{ON} = S^+_{ON} + S^-_{ON}$$
$$Y_{OFF} = S^+_{OFF} + S^-_{OFF}$$
$$\mathcal{A}_{ON} = \frac{\Delta_{ON}}{Y_{ON} - \langle Y_{OFF} \rangle}$$
$$\mathcal{A}_{OFF} = \frac{\Delta_{OFF}}{\langle Y_{ON} \rangle - \langle Y_{OFF} \rangle}$$

$$\mathcal{A}_{exp} = \langle \mathcal{A}_{ON} \rangle - \langle \mathcal{A}_{OFF} \rangle = \mathcal{P}_e \mathcal{P}_\gamma \langle \mathcal{A}_l \rangle$$

With laser DOCP $\mathcal{P}_\gamma$, energy-weighted average analyzing power $\langle \mathcal{A}_l \rangle$, and beam polarization $\mathcal{P}_e$.

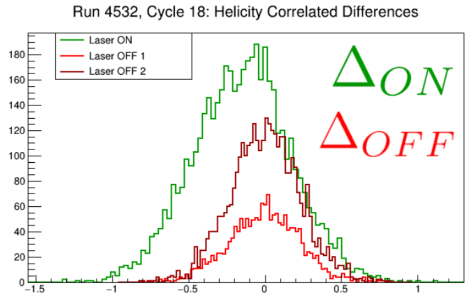

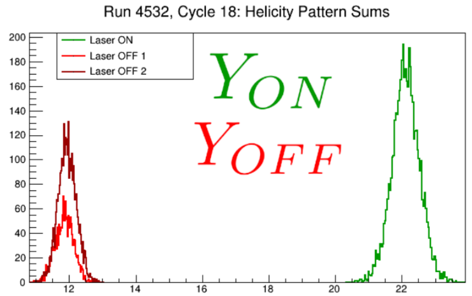

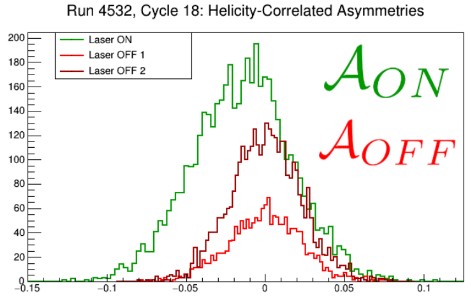

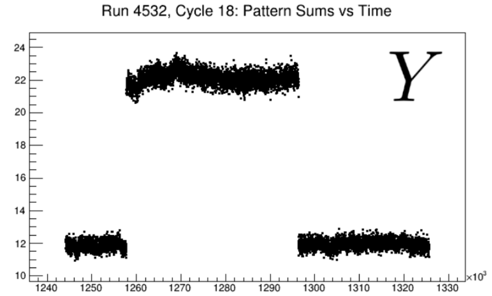

A. Zec Thesis: DOI: [10.18130/xpq1-7090](https://doi.org/10.18130/xpq1-7090)

Compton spectra

- Typical Compton spectrum was well characterized by simulations
- Measurements during data collection on the lead target showed a very large background from thermal neutrons

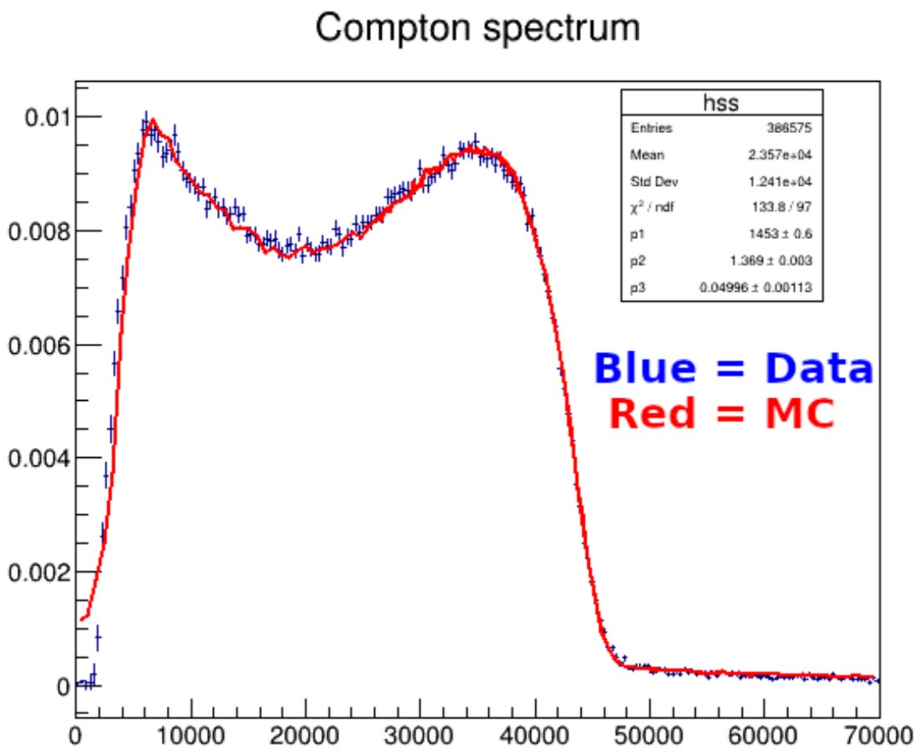

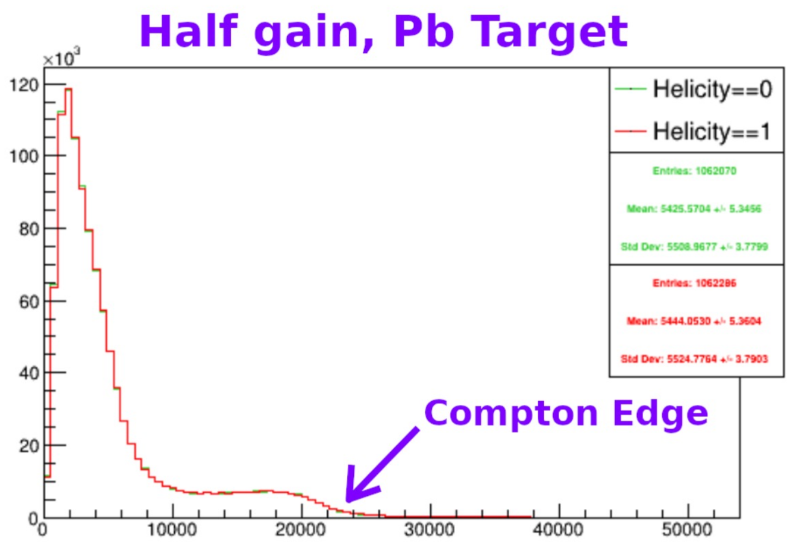

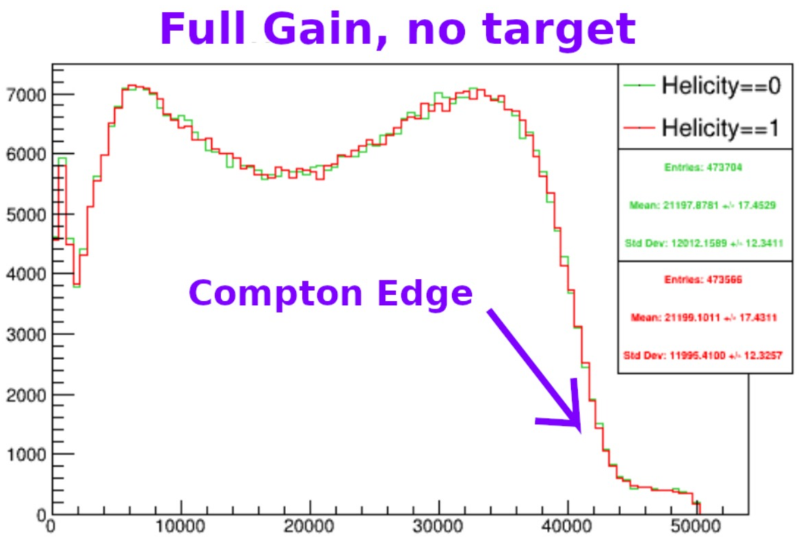

A. Zec Thesis: DOI: [10.18130/xpq1-7090](https://doi.org/10.18130/xpq1-7090)

Combined results

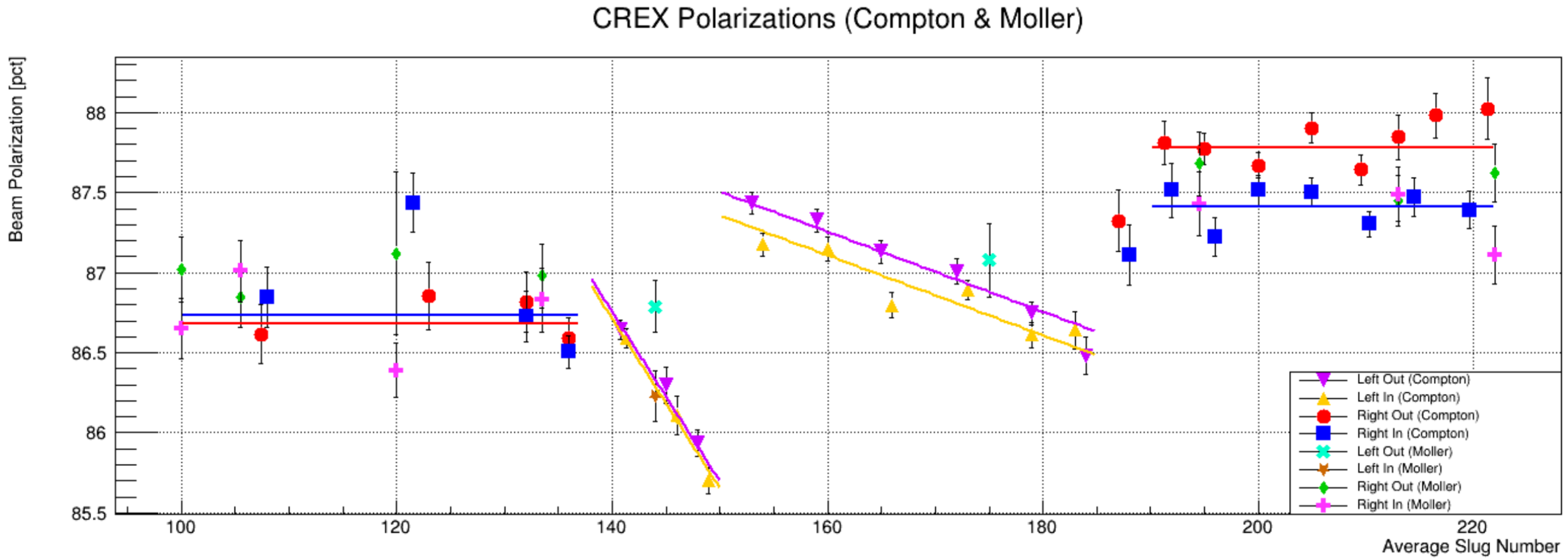

Above: Møller and Compton polarimetry data for CREX. All uncertainties plotted are statistical only. Moller data courtesy of E. King.

$$P_{\text{beam}} = (87.10 \pm 0.39)\% \qquad \frac{\Delta P_{\text{beam}}}{P_{\text{beam}}} = 0.45\%$$

A. Zec Thesis: DOI: 10.18130/xpq1-7090